Dextrous robotic hand with multi modal sensing

Mechanical design and prototype manufacturing

Author:

Shannen Venethethan

Student ID: 210478226

Project Supervisors / Advisors:

Dr Ketao Zhang

Dr Arsen Abdulali

Jianlin Wang

Chen Liu

Group 239 Members:

Richard Somovidis: 221115000

Sahimaa Surenthiran: 220283225

Seagull Nithyanandam Vennila: 220454043

April 2026

I. Abstract / Executive Summary

This report outlines the mechanical design, manufacture and evaluation of the mechanical work package for the Dextrous Robotic Hand with Multimodal Sensing project. The main goal of this study was to develop a low-cost and research-ready robotic hand platform which is capable of supporting tactile sensing and reactive motion. The original strategy was to adapt the open-source ORCA hand however, the published CAD files were not sufficiently editable for the required sensing, actuation and packaging changes. The individual work package therefore moved to an completely original mechanical redesign while retaining ORCA as a benchmark.

The final prototype consisted of two fully actuated fingers, two underactuated fingers and one fully actuated thumb. The design features split phalanx assemblies, tendon anchors, 3D printed torsion springs, carpal tendon routing, removable sensing fingertips, detachable motor hub and mounts for the Raspberry Pi 5 and OpenCR. The prototype was FDM 3D printed in PLA and assembled using bearings, heat-set inserts, M2 and m3 hardware, nylon tendons and DYNAMIXEL actuators.

The completed prototype showed that the CAD architecture could be manufactured, assembled and integrated into a serviceable robotic hand. Initial preliminary assessments demonstrated that movement occurred in the correct direction with successful integration of sensors into the fingertips. Further quantitative evaluation is needed with respect to validly established grasping forces, backlash, fatigue life and long term PLA performance.

II. Contents page

III. List of Figures and Tables

Figures

Tables

IV. Nomenclature

TABLE 1: Nomenclature

Term	Definition
A1	Bambu Lab A1 FDM printer
A1 Mini	Smaller Bambu Lab FDM printer
CAD	Computer Aided Design
CBOM	Costed Bill of Materials
COTS	Commercial Off TheShelf
DOF	Degree of Freedom
DP	Distal Phalanx
FDM	Fused Deposition Modelling
FEA	Finite Element Analysis
FSR	Force Sensitive Resistor
M2/M3	Metric thread sizes used in the prototype assembly
MCP	Metacarpophalangeal joint
MP	Middle Phalanx
OpenCR	ROBOTIS control board used to interface with DYNAMIXEL actuators
PLA	Polylactic Acid FDM printing material
PP	Proximal Phalanx
ROM	Range of Motion
ROS	Robot Operating System
STL	Stereolithography file format
STEP	Standard for the Exchange of Product Data CAD file format

V. Declaration of Own Work

I declare that this individual report is my own work and represents my own contribution to the MEng Team Project, Dextrous Robotic Hand with Multimodal Sensing. The work reported here focuses on the mechanical design, manufacture, assembly and evaluation of the robotic hand prototype.

I designed the mechanical CAD redesign with respect to tendon routing, split phalanx structure, tendon anchors, under-actuated fingers, printed springs, carpal assembly, motor hubs, the mechanical integration features for accommodating sensors, manufactured prototypes and mechanically integrated them myself. Other team member contributions are also noted throughout the report with regards to development of software/ROS, electronics integration, actuation control and wiring/fingertip sensing.

The work presented here is based on literature mainly published papers, manufacturers information, software documentation and open source designs. All of these outside references are identified within the report with citations. While the ORCA hand was a starting point for benchmark and design inspiration, the mechanical configuration discussed in this report represents a complete redesign of the hand. This is because the available CAD files for the ORCA did not lend themselves easily to conversion/adaptation into our desired mechanical configuration.

This report has been authored truthfully. The results, limitations and conclusions represent accurately what was found during completion of this project. Any use of software tools, including CAD software, diagramming tools and grammar-checking tools, was solely for the purpose of improving the development, clarity and presentation of the report, and does not misrepresent my role in carrying out the engineering work.

Name: Shannen Venethethan

Student ID: 210478226

Date: 29/04/2026

Signature:

VI. Acknowledgements

I would like to thank my project supervisor, Dr Ketao Zhang, for his guidance, technical advice and continued support throughout the MEng project. His feedback was particularly valuable during the development of the mechanical design, including decisions around the CAD redesign, tendon routing and under-actuated finger arrangement. I would also like to thank Dr Arsen Abdulali, Jianlin Wang and Chen Liu for their support during project meetings, design discussions and technical reviews.

I would also like to acknowledge my team members, Richard Somovidis, Sahimaa Surenthiran and Seagull Nithyanandam Vennila, for their contributions to the wider project across mechanical design, sensing, electronics, software/control and system integration. Their collaboration helped support the development of the robotic hand prototype as a complete multidisciplinary system.

1. Project Background and Work Package Flowchart

1.1 Project Background

The goal of the Team Project, Dextrous Robotic Hand with Multimodal Sensing, was to create a research ready, low-cost robotic hand platform that combines dexterity, tactile sensing and control system integration. Initially, the focus of the project was to adapt the open-source robot ORCA hand[1] which has a multi-tendoned, tendon driven design that provides an anthropomorphic hand shape and includes tactile sensor capability as well as relatively low deployment costs. Anthropomorphic, tendon driven hands have been extensively researched due to their ability to provide humans like capabilities and provide dexterous manipulation but also increase the difficulty in designing and controlling them when compared to simple gripper designs[1], [2].

The project addresses a significant engineering gap. Typically, robotic hand design is constrained by a trade-off between simple, low-cost grippers that lack dexterity or increasingly complex. Anthropomorphic hands that attempt to achieve increased dexterity at the expense of significantly higher complexity and cost through more actuators, sensors and mechanical components[2], [3]. Additionally, successful hand platforms require not only the ability to generate motion but also provide the capability to sense the environment because grasping and interacting with objects requires both actuation (motion) and feedback (sensing)[3]. As early as the first week of development, the mechanical stream identified a practical CAD constraint within the source files of the ORCA hand. This led to a redirection of focus from adapting an existing design to a complete redesign of the hand while maintaining the overall goals of the larger project.

1.2 Project Rationale, Aims and Objectives

This project aimed to design a robotic hand platform that combined tendon driven actuation, multiple sensor types, module integration, and the ability to interface with future control architectures. A key benefit of using tendon based systems is that it allows actuators to be placed remote from the links that move which will typically reduce both the inertial loads on those links as well as the mass associated with them[4]. At the same time, underactuated and modular hand structures have been shown to be beneficial due to their lower number of actuators, reduced weight and lower overall complexity while maintaining sufficient grasp capability[5], [6].

Therefore, in developing a robotic hand capable of providing a framework for sensors, electronics and software along with hand functionality, the objective was to produce a modular tendon-based hand capable of integrating various types of sensor hardware; incorporating embedded electronic components; and having geometric configurations ready for use by software. This goal aligns with the purpose of open source research hands, which emphasize modularity, cost-effectiveness and ROS compatible development environments[7].

1.3 Teamwork Allocation

TABLE 2: Teamwork Allocation

Team member	Primary responsibility	Scope of contribution
Shannen	Mechanical design and manufacturing	Full mechanical CAD redesign, additive manufacture, assembly, subsystem accommodation and software-ready geometry export
Richard	Software, ML and ROS	Simulation workflow, ROS integration and control development
Seagull	Electronics	Wiring architecture, power and actuator interfacing
Sahimaa	Fingertip sensing	Sensor dimensions, placement and sensing integration requirements

1.4 Individual Work Package

The original plan was to modify the ORCA hand to accommodate the project's sensing and actuation needs. As this was not possible, the work expanded to full hardware redesign, including CAD development, tendon routing, underactuated finger design, thumb simplification, modular fingertip design, fabrication planning, physical assembly and software-ready geometry export.

1.5 Individual sub-RAO

Develop and manufacture a modular tendon-driven robotic hand structure in order to support the aims of the overall project. The design has to integrate sensing, electronics and software into the physical design of the robot.

This work package involved design iteration around printability, tendon routing, assembly access, subsystem accommodation and serviceability. The intended output was a full buildable mechanical system, not just a collection of CAD parts.

The realised mechanical package enabled the other members of the team to develop their respective elements of the project. For example, the developed routing strategy for the tendons, modular fingertip modules, under-actuation of finger movements and packaging of motors/electronics were all influential in how sensing was incorporated into the system, where electronics were located within the system and where software testing could be undertaken on the final prototype.

1.6 Work Package Flowchart

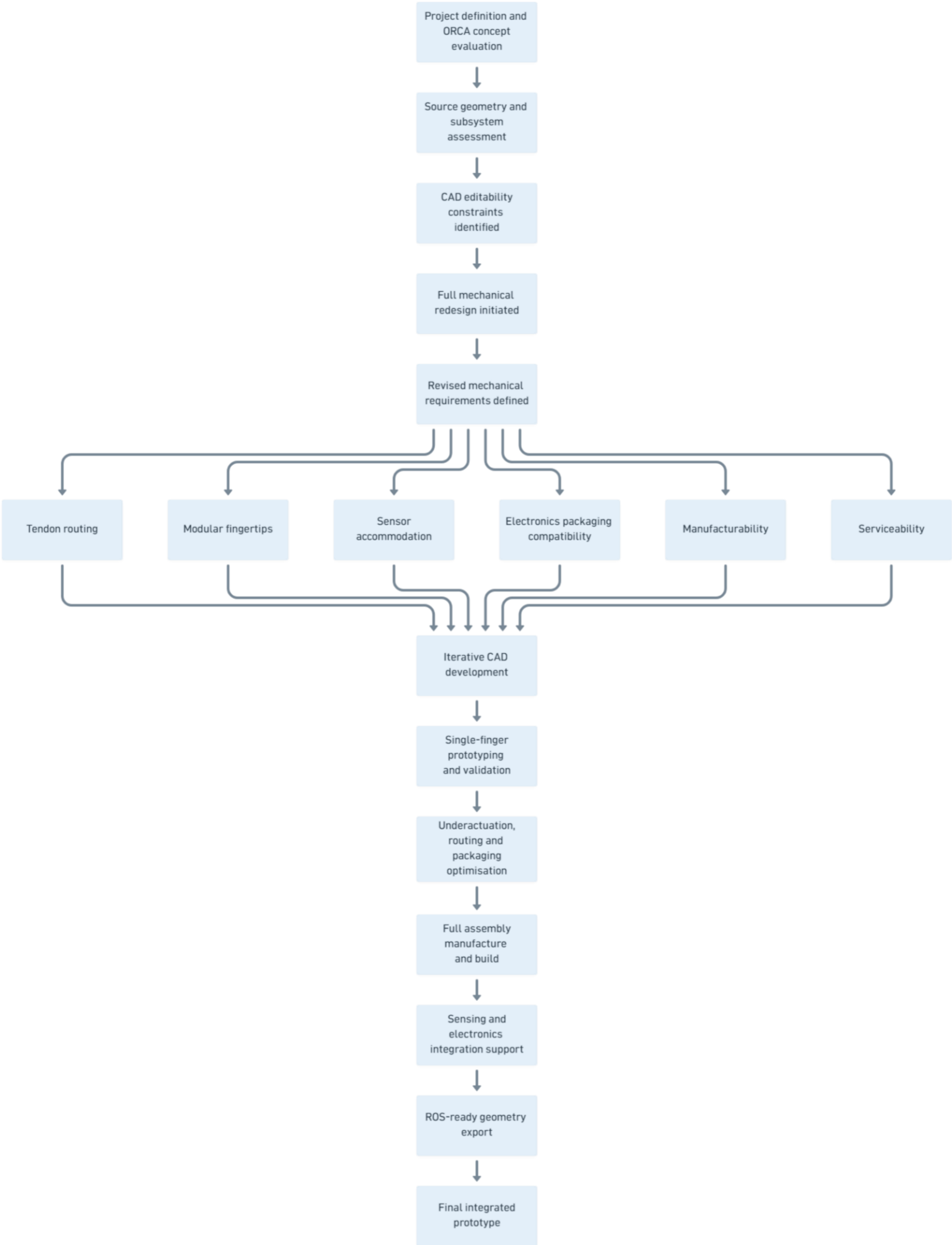

FIG 1: Project flowchart crated with Whimsical [8]

2. Literature Review

2.1 Open-source anthropomorphic robotic hands as baseline systems

There are few open-source anthropomorphic robotic hands that simultaneously meet the requirements of dexterity, affordability, reliability and ease of deployment. Majority of the current designs improve upon one or two of these requirements while compromising others [2]. many dexterous hand prototypes have been developed, however most of them end up as laboratory specific or prototypes because they have not bridged the manufacture, assemble, maintain or/and reproduce reliably [2] gap. The reason ORCA was created was to develop an open-source, anthropomorphic hand design that would be easy to make, affordable, capable of repeatable performance and durable, provide good tactile sensing and could be assembled quickly. In this way ORCA provides a particularly suitable reference point since it has all of these features combined into one low-cost (<2000 CHF) open-source research platform [1]. ORCA's joint popping, automatic calibration and its ability to tighten its tendons also demonstrate a greater focus on repeatability and durability compared to many earlier open-source hand projects [1].

The ORCA hand relies on complex tendon routing and high level actuation, all characteristics that continue to limit the ease of integration [1], [9]. HRI Hand offers a cheaper, modular, underactuated alternative with ROS support but is less functional and has less built-in sensing than ORCA [7]. ALARIS represents a further improvement in terms of price and structural robustness when compared to ORCA, however it loses some of ORCA's capability and sensor readiness [9]. Previous 3D-printable hand examples were able to increase access to robotics technology but had more limited scope than the present project [10].

FIG 2: Orca Hand reproduced from [1]

2.2 Under actuation in robotic fingers and hands

Due to its potential to reduce actuator count, weight, cost and control complexity while increasing shape-adaptive grasping capabilities, underactuation has been adopted in many robotic fingers/hands [11], [12]. The greatest benefit of underactuation occurs when the primary objective is reliable grasping and not full dexterous manipulation. In fact, underactuated fingers have shown great success in enveloping objects and distributing forces utilizing simple control schemes [11].

However, there are corresponding disadvantages including reduced independent joint control, decreased precision in finger motions and limited manipulation abilities [11], [13]. Any successful underactuated design must meet criteria like those required for natural motion, stability, compactness and force transmission requirements. Furthermore, underactuated designs cannot simply treat motor reductions as advantages without compromising one or more of these necessary criteria [14].

2.3 Tendon-Driven Finger Coupling and Routing

Tendon-driven hands allow actuators to be positioned away from the moving joints, reducing local link mass while supporting flexible routing and anthropomorphic finger layouts[4], [15], [16]. However, the literature has shown that tendon systems are highly dependent upon routing geometry, pulley position, friction, slack, and hysteresis; therefore, there is difficulty in accurately modeling and achieving consistent performance [4], [15], [17]. Studies examining individual fingers demonstrate that the arrangement of tendons and changes in moment arm lengths can intentionally produce coupled motion between joints and significantly affect the transmittal of forces [15], [17]. In addition, hand-level studies have demonstrated that optimization of pulleys can improve efficiency; however, this can add additional mechanical complexities to the system [15], [17].

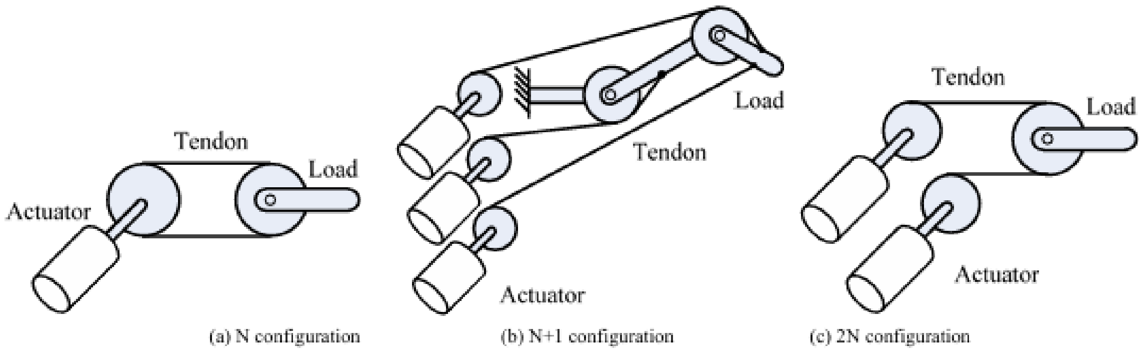

FIG 3: Types of tendon-driven robotic mechanisms reproduced from [16]

2.4 Anthropomorphic Geometry and Motion Constraints

The selection of joint geometry for the design of an anthropomorphic hand is based on choosing functional geometry as opposed to simply replicating anatomy [18]. The literature demonstrates that thumb orientation, opposition, joint axes, and finger shape greatly impact grasp stability, workspace, and natural motion [18], [19]; therefore, simplification of these characteristics may be required, due to difficulties associated with modeling, manufacturing, and controlling biologically accurate joint configurations [18], [20]. Therefore, these papers are useful for explaining why robotic fingers typically require constrained motion paths and why thumb kinematics are most commonly simplified to achieve repeatable grasps which are stable as opposed to completely anatomically accurate.

2.5 FDM 3D printing for Robotic Hand Structures

3D printing provides several attributes that make it suitable for anthropomorphic hands including rapid iterations of designs, complex geometries, consolidated parts, customizations, and low-cost prototyping [21], [22]. Additionally, 3D printing enables the creation of compliant, monolithic, and hybrid rigid-soft structures which can decrease assembly complexity and weight while increasing grasp adaptability [21], [23] . However, the literature clearly identifies specific limitations: printed parts can exhibit uncertainty regarding their mechanical properties; material options are limited; processing parameters can increase sensitivity to accuracy; and there is no guarantee that printed parts will be durable over time under actual use conditions [23], [24]. These issues are directly related to both the design and testing of a printed hand.

2.6 Heat set inserts in 3D Printed Parts

Heat-Set Inserts for repeated assembly can provide a reusable metal thread within a printed component as opposed to the traditional method of printing a threaded hole using plastic [25]. However, joint reliability is determined by the geometry of the printed part such as infill density and layer bonding therefore, the surrounding printed structure may fail prior to the failure of the insert bond [25].

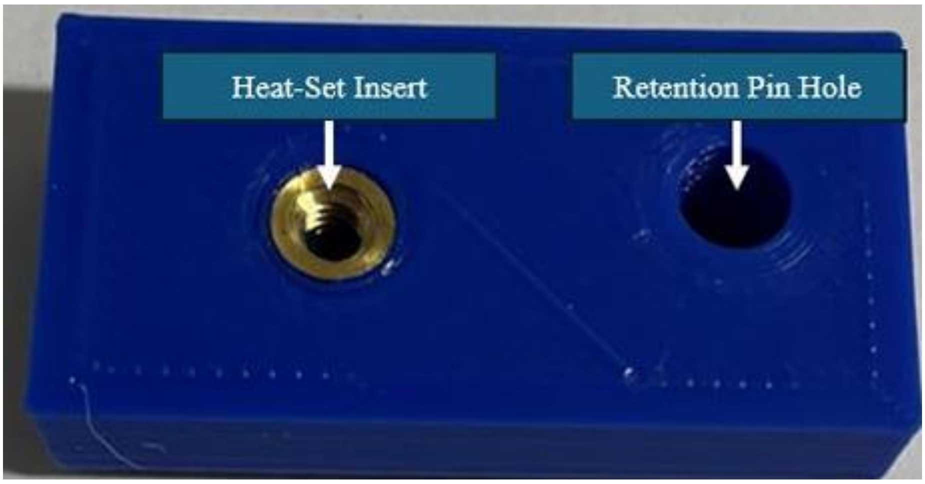

FIG 4: Example of heat-set insert in a 3D printed part reproduced from [25]

2.7 Compliant Passive Elements and 3D Printing

3D printed springs are attractive for being inexpensive to build, simple to construct, easily replaced and can be integrated directly into compliant mechanisms with decreased assembly complexity [26], [27]. The literature also indicates that their geometric configuration can be optimized for predictable stiffness and even precision motion control [26], [28]. However, such benefits rely heavily on proper parameterization of printed spring design and quality of prints; as well as specified operational ranges because excessive friction; parasitic motion; hysteresis; and fatigue can negatively affect both the accuracy and longevity of 3D printed springs [26], [27]. Therefore, printed springs are viable compliant passive elements, yet are not performance neutral alternatives for traditional components.

2.8 Modularity, serviceability and integration with sensors

Modularly integrated touch is beneficial due to the fact that individual sensor components can be customized to fit a variety of fingertip geometries; they may be calibrated away from the hand and easily be replaced if damaged, which reduces the need to completely dismantle other structural components in the system [29], [30]. Additionally, literature has shown that modular designs provide improved access to both maintenance and iterative development, especially when fingertip volume and/or surface geometry restricts the integration process [29]. Although the above factors increase the ability to replace/perform service on individual tactile components of the hand (modularity) this does not eliminate the main challenges associated with tactile based systems. The reliability and scalability of those systems will continue to depend upon a number of factors including, wire routing issues, packaging space constraints, mechanical robustness, and signal stability [31]. Therefore, the primary benefit of modularity is increased replacement/serviceability, as opposed to a simpler integration process.

3. Mechanical Design Methodology and Iterative Development

3.1 Introduction and Mechanical Design Strategy

SolidWorks software[32] was used to develop the mechanical design. A top-down CAD methodology was implemented, which allowed for the design of all components (finger geometry, path of the tendons, sensor location, carpal routing and motor placement) in relationship to the entire hand before developing each component. After the overall geometric layout was determined, the design was separated into smaller, printable sub-assembly units to allow for better print orientation, access to internal designs and serviceability.

A primary goal of this design effort was to create a fully operational FDM prototype rather than simply creating a visual CAD model. Clearance dimensions were set at a minimum of 0.2 mm for all typical fits, although clearance dimensions ranging from 0.2 mm through 0.5 mm were applied wherever increased friction would result due to contacting surfaces on moving parts, tendons or bearing interfaces. Rotating joints utilized 1063ZZ bearings and all other major printed assemblies were designed to utilize consistent fasteners M3, with heat-set inserts. Screw holes, insert holes and bearing holes were oversized when necessary to ensure reliable assembly and minimize damage to printed plastic caused by repeatedly assembling and disassembling the various sub-assemblies. Assessments of design iterations included evaluation of CAD mates, prints, manual inspection of tendon routing and assessment against system requirements and advice from advisors. A design iteration was deemed acceptable upon demonstration of the ability to successfully print, assemble, demonstrate movement as desired, provide clean tendon routing and reserve adequate space for sensors and electronic systems.

3.2 Initial concept development and ORCA adaptation

Initially the plan was to take the open-source ORCA [1] hand as a base model, in order to use its scale, tendon-based mechanism and carpal routed design as a foundation for development. Using this method would have greatly reduced some of the risks associated with early design decisions. However, upon reviewing the source files of the ORCA hand, this direction proved to be unfeasible. First, the provided STEP file did not lend itself well to parameterization. Second, when importing STL files which is the format used by 3D slicing software the resulting assemblies often contained voids or "hollow" areas which could not be successfully translated into solid bodies. In addition to studying motion through printing two ORCA style fingers; there was additional benefit derived from studying how tendons are routed. While this exercise provided insight into the mechanics involved, it further illustrated that the routing of tendons and the placement of sensors at the tip of the finger would require much less complex designs than those presented in ORCA. Thus, rather than utilizing ORCA as a basis for the final design, the project shifted to an original redesign, while retaining ORCA as both a benchmark and to adapt selected existing geometries.

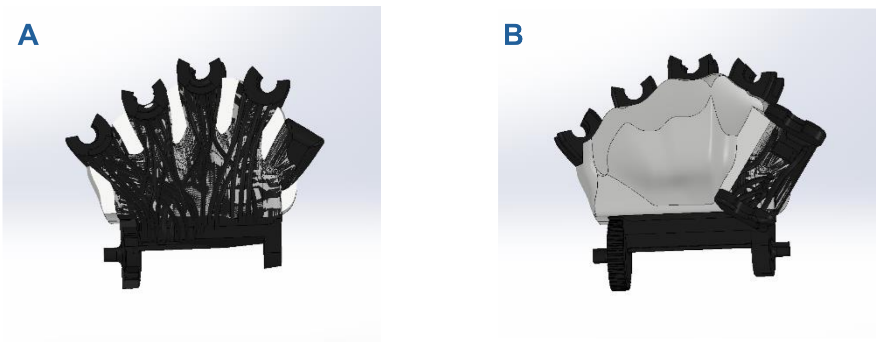

FIG 5 (A&B): ORCA hand reproduced from [1] imported STL into SolidWorks [32]

3.3 Tendon anchor

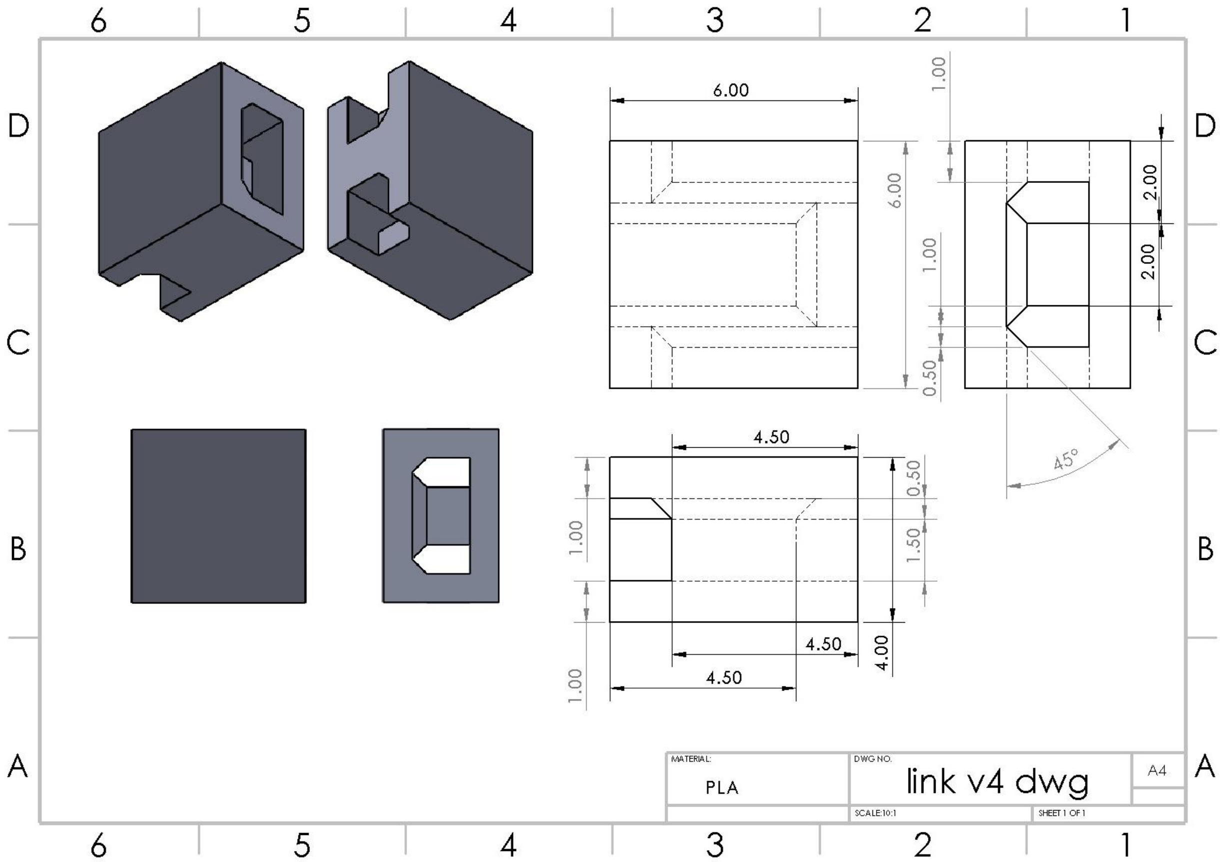

FIG 6: Tendon anchor (Link v4) technical drawings

A tendon anchor was created to secure the nylon actuator wires at each of the mobile phalanx sections. Alternative anchor concepts would have required clamps or adhesive, so a printed knot-retention feature was developed instead. A unique bidirectional knot retention method was finally employed; the wire was passed through a small channel, tied into a knot and seated inside a recessed pocket. Due to the fact that both channels on either side of the pocket are smaller than the knot itself, this prevents the tendon from being pulled out in either direction.

Because the geometry allows for bidirectional tendon loading with little backlash, the knot is positioned under the exterior surface. Additionally, the recess prevents the tendon path from interfering with neighbouring elements such as tendons and joints. The previous versions of the tendon anchors were discarded for several reasons. They were much more difficult to print than their predecessor and many of them broke early in testing as a result of poor local geometric strength. The final version was easier to print and remained functional during testing. It was ultimately compatible with all the other parts of the final finger assemblies.

3.4 Fingertip design (DP)

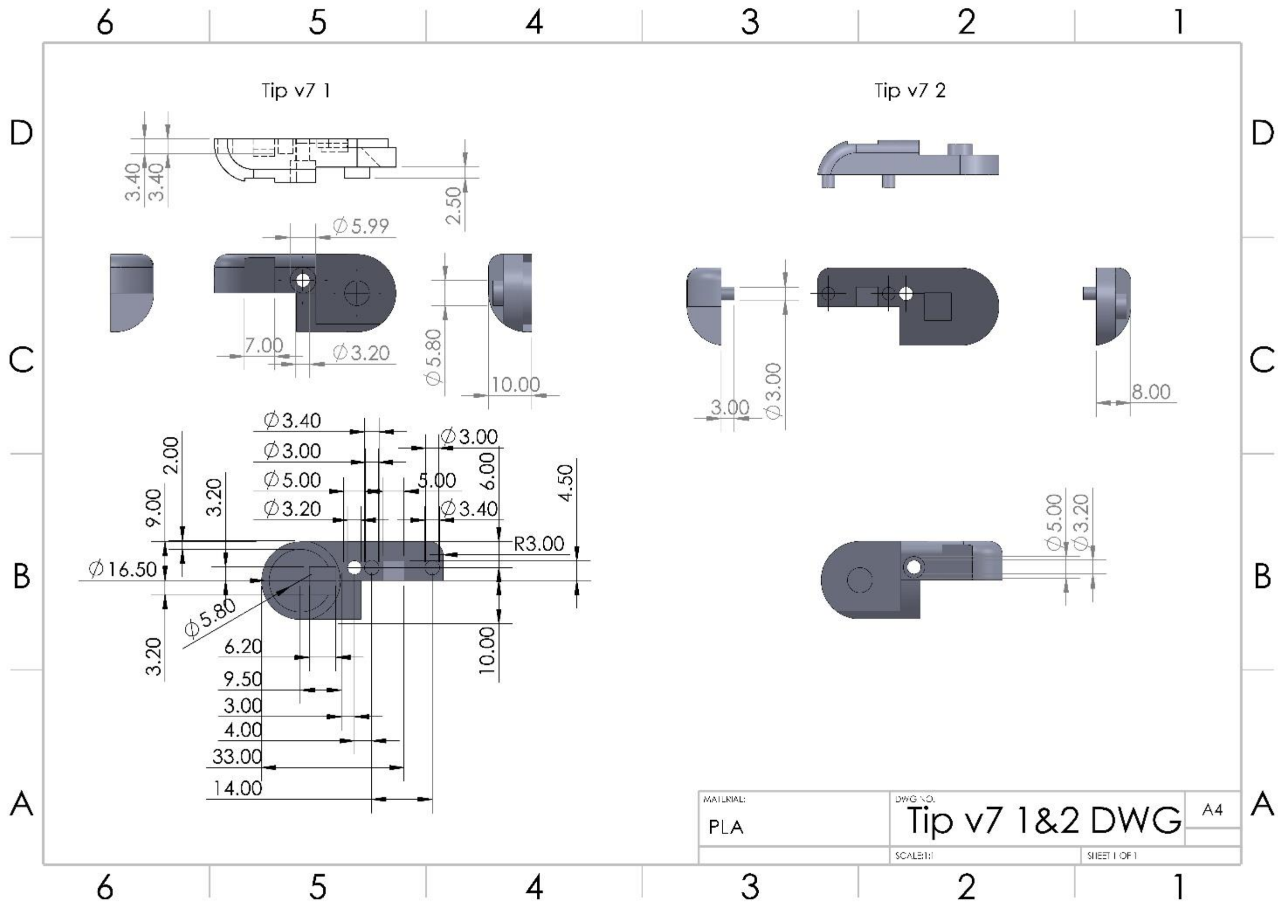

FIG 7: Tip V7 1&2 technical drawings

The final distal phalanx section was broken down into two separate printed pieces (V7 1 & V7 2). Although these two printed pieces are referred to as Tip V7 1 and Tip V7 2, they are not separate design options. Rather, they represent two different printed parts which will eventually become one single fingertip after being assembled. Splitting the fingertip into two printed parts allowed the internal tendon path and anchor geometry to be manufactured and assembled more reliably.

Tip V7 1 includes most of the main tendon channel and anchor geometries and therefore keeps the tendon path contained to only one part rather than spanning multiple parts across a joint that may exist between printed parts. Tip V7 2 completes the structure and avoids any potential conflict with the tendon path. In addition, by keeping the tendon route within one printed part, there is less chance for the tendon to slip into an opening in the assembly and therefore improves overall reliability of the tendon routing. The designs also included additional features such as fastening screws, joints and clearances to ensure consistency in manufacturing the fingertip as opposed to considering it solely as a CAD concept.

3.5 Fingertip module and mould negative

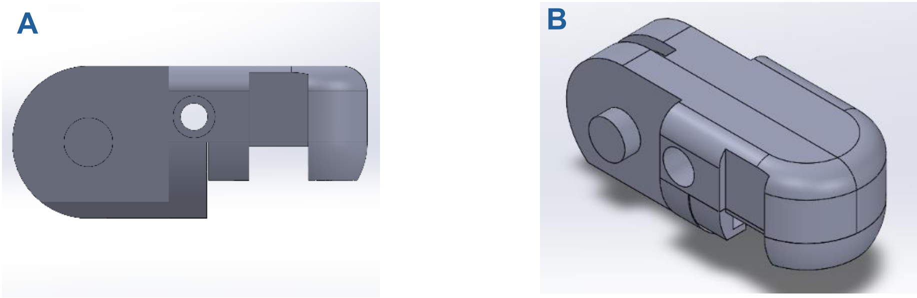

FIG 8 (A&B): Side and orthogonal view of final tip assembly

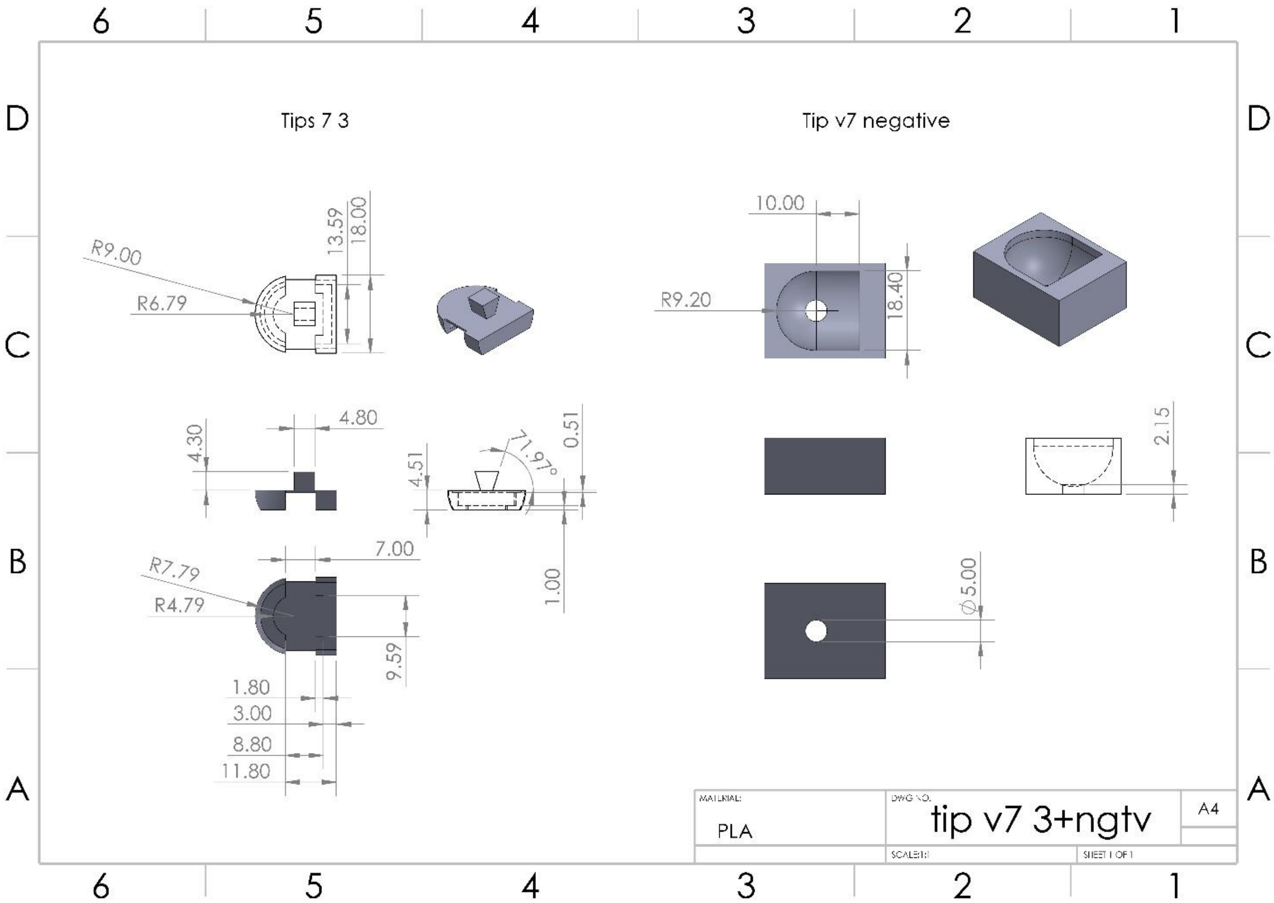

FIG 9: Tip V3 and mould negative technical drawings

The removable fingertip sensing system employed a Tip V7 3 insert and separate mould negative. The Tip V7 3 insert was fitted into the structural fingertip and was dimensioned so that it would fit an FSR sensor with a maximum diameter of 6 mm. The Tip V7 3 insert can be removed from the structural fingertip using the same method of attachment that is described in section 3.1 to replace or calibrate without having to remove the entire fingertip. The Tip V7 3 also functioned as a solid foundation for the compliant silicone sensing pad. To create the base layer of silicone for the sensing pad, the hollow area of the insert was first filled with silicone. Next, the FSR sensor was placed onto this layer, followed by placement into a mould. Afterward, additional layers of silicone were poured into the mould until fully cured. The mould defined the outer surface of the soft fingertip. In addition to creating a mechanical retention mechanism for the silicone in terms of lip features on the insert, these features also reduced dependence upon adhesives. As such, the fingertip design provided both sensor compatibility and the ability to provide maintenance service to the finger.

3.6 Middle Phalanx Design (MP)

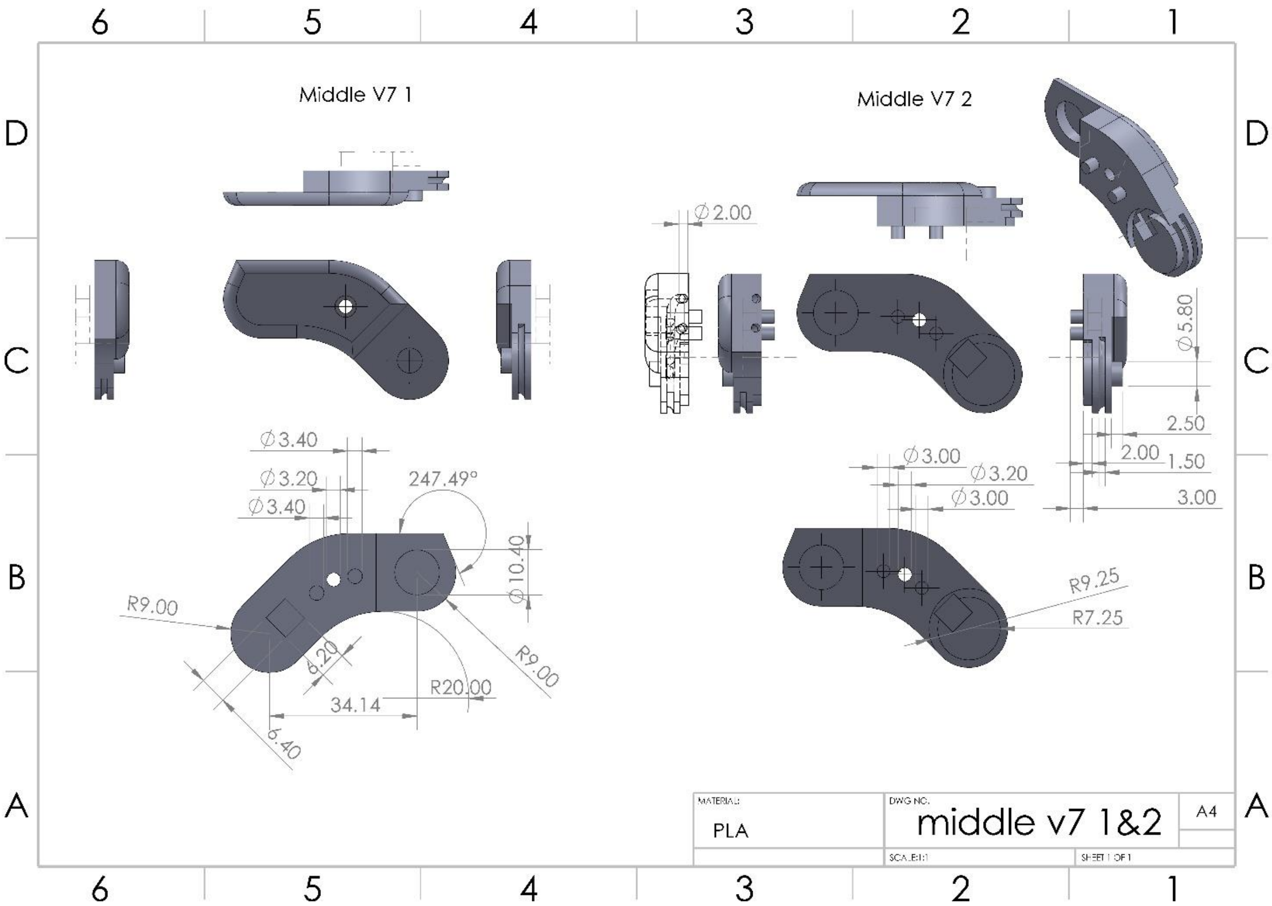

FIG 10: Middle V7 1&2 technical drawings

The middle phalanx was split into Middle V7 1 and Middle V7 2 to make the internal tendon anchor and routing features printable and accessible. Middle V7 1 is the smaller component and supports the pin locations, while Middle V7 2 carries the main tendon-routing channels and anchor pocket. This split also improved serviceability because one worn half could be replaced without discarding the whole phalanx.

The final geometry incorporated hard stops to control the motion envelope. The joint allows approximately 90° forward flexion and 45° backward extension, giving a total range of about 135°. The backward allowance lets the non-thumb fingers return to a flat posture, while the stop prevents over-rotation. Three separate tendon routes were included to keep tendon paths organised and reduce unintended coupling between lines.

3.7 Proximal/end segment design (PP)

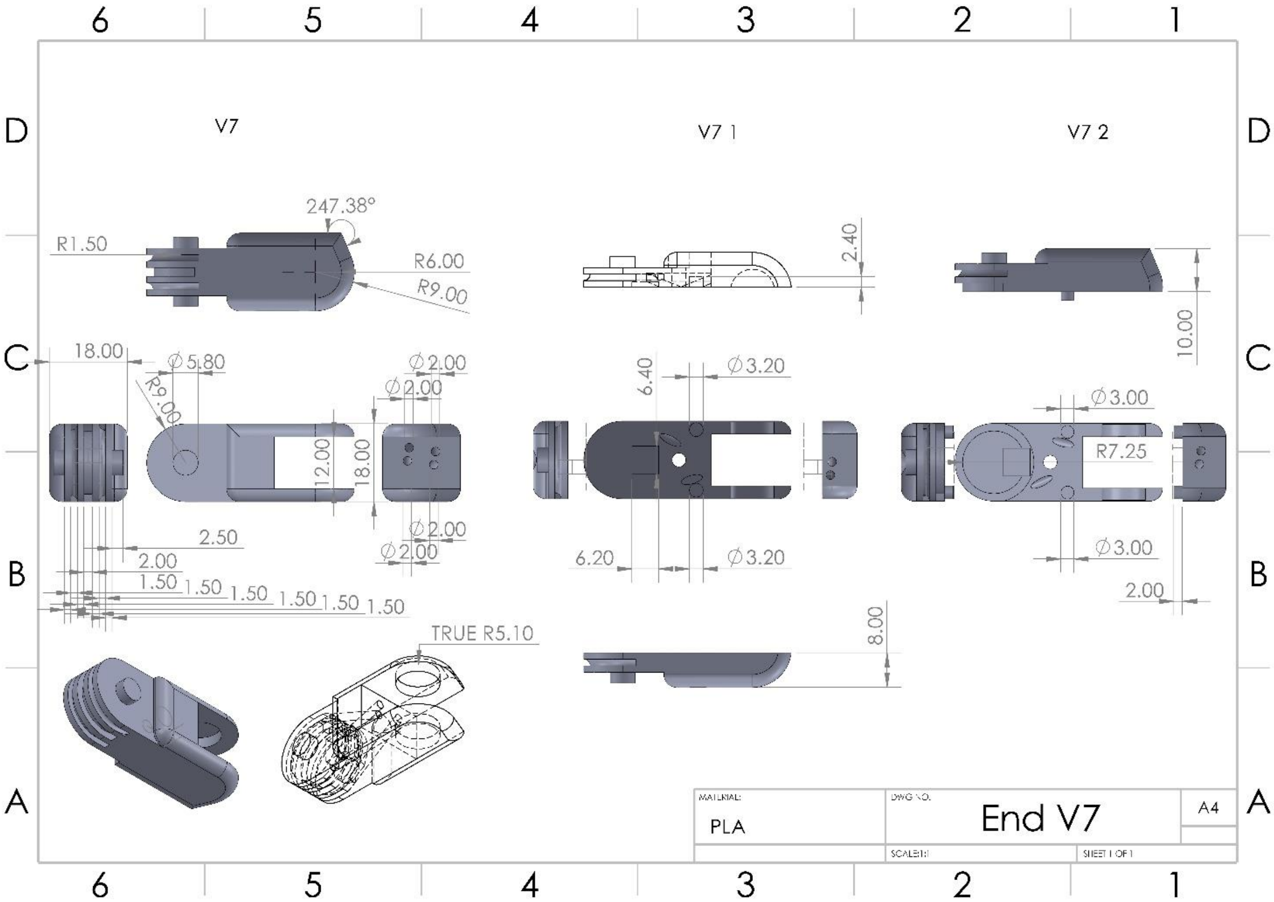

FIG 11: End V7 technical drawings

The proximal/end segment connects the finger phalanges to the carpal structure and changes the motion direction from front–back bending to side-to-side motion at the carpal-facing joint. The geometry allows for 60° of side-to-side motion at the carpal interface while still supporting the 90° flexion and 45° extension.

The bottom hard-stop of the proximal segment will contact the carpal structure; thereby enabling the finger to lie flat against the surface while limiting excessive extension. The V7 2 includes the tendon-anchor and has three tendon-routing channels which maintain separation of the tendons as they go through each channel. To maintain consistency throughout the entire hand assembly, this section utilizes the bearing-supported carpal interface discussed in Section 3.1.

3.8 Thumb Segmented Design and Joint Simplification (T-MP/T-PP)

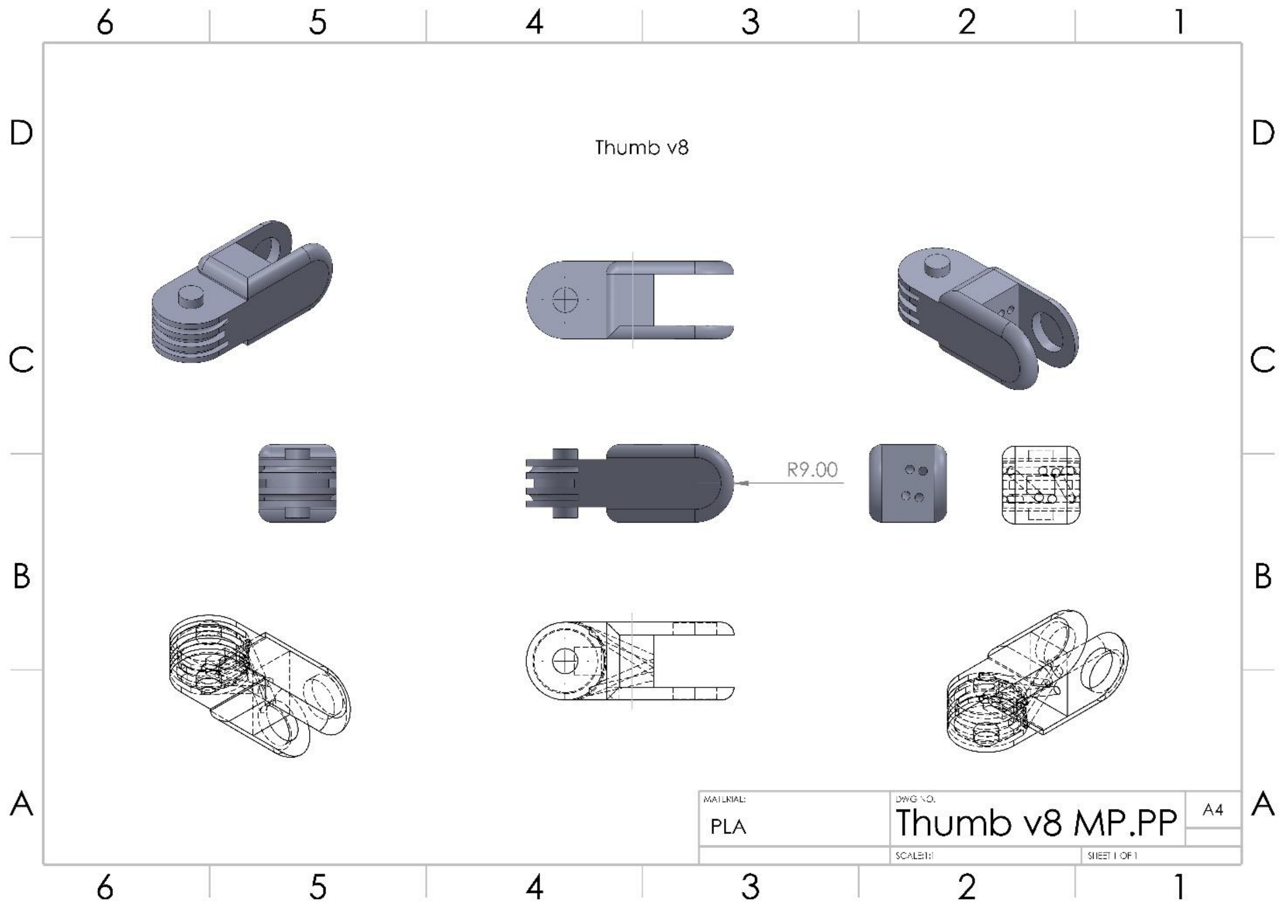

FIG 12: Thumb v8 MP.PP technical drawings

To reduce the number of printed parts and improve servicing capabilities, the thumb incorporated the Thumb V8 MP.PP segment twice along with its own thumb-tip segment. Each printed part can be used in either thumb-position, reducing the total number of unique printed parts. In comparison to the End V7,this part is very similar; however, since it does not have any hard-stops, it enables greater flexibility when adjusting the thumb's positioning.

The thumb's kinematic movement was greatly simplified by separating the opposition into two simpler joint motions as opposed to developing a single multi-axis joint that encapsulated all of these movements. The first segment close to the carpal causes the thumb to extend toward the little finger while the second segment causes it to extend toward the index finger. This allowed the hand to simulate opposition while maintaining a simple, modular and consistent printed geometry with the remainder of the hand.

3.9 Under actuation Spring

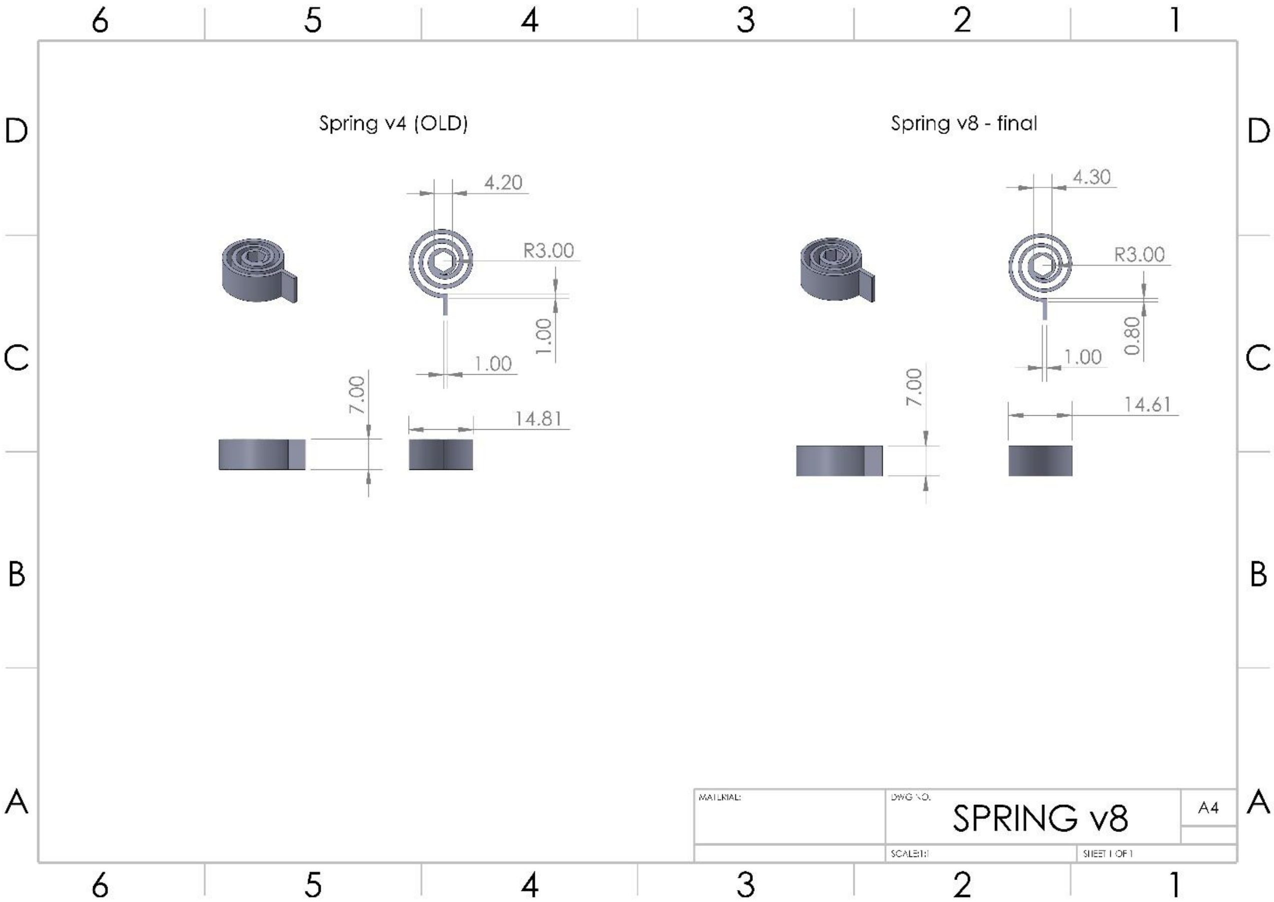

FIG 13: Old and final Spring V8 technical drawings

An underactuated spring used a small 3D printed coil with an internal hexagonally shaped feature. Therefore, the spring could be placed on the matching joint surface providing a low-load, passive return torque. A previous design was overly rigid therefore, to enable tendon driven movement while maintaining some return action, the wall thickness of the final Spring V8 was decreased from 1.00 mm to 0.80 mm.

A larger hexagonal groove internally was created from 4.20 mm to 4.30 mm to help assemble the unit. A replaceable printed spring for use in prototype development has been developed; however, its durability over time is still being tested by long term fatigue tests.

3.10 Underactuated Fingertip (DP)

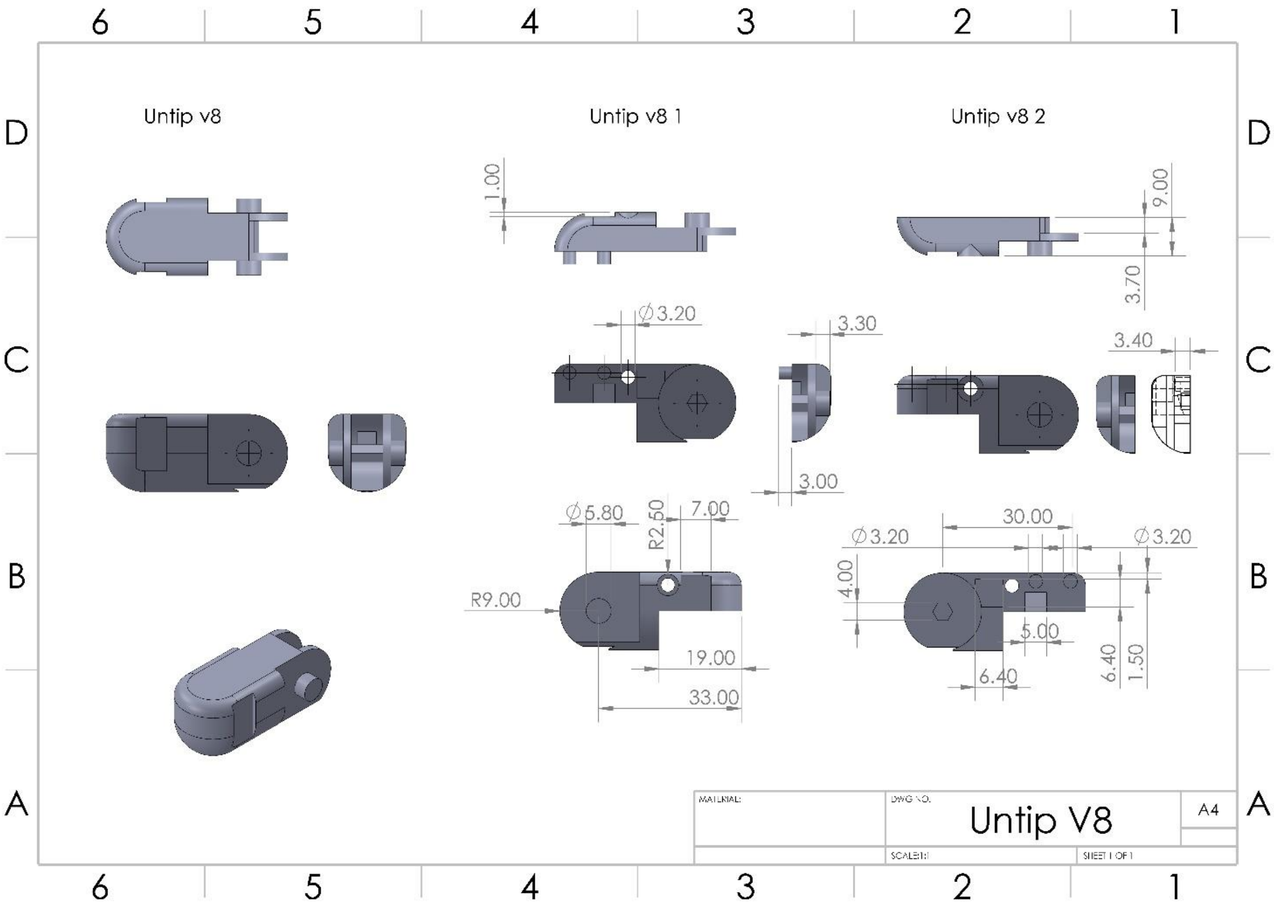

FIG 14: Utip V8 technical drawings

The underactuated tip has two separate parts, Untip V8 1 and Untip V8 2. While retaining the same overall shape as the fully actuated fingertip, the anchor point of the tip was raised to accommodate the mounting position of the spring. Since the tendon can sit externally of the spring, the part was split in half to fit the modified internal arrangement of the parts. Untip V8 1 will have locating features to allow proper alignment of Untip V8 2. As in all other units, a single method of fastening was used which ensures ease of maintenance and serviceability should wear occur in the spring seat, tendon path, or anchor area during testing.

3.11 Underactuated middle and end (MP/PP)

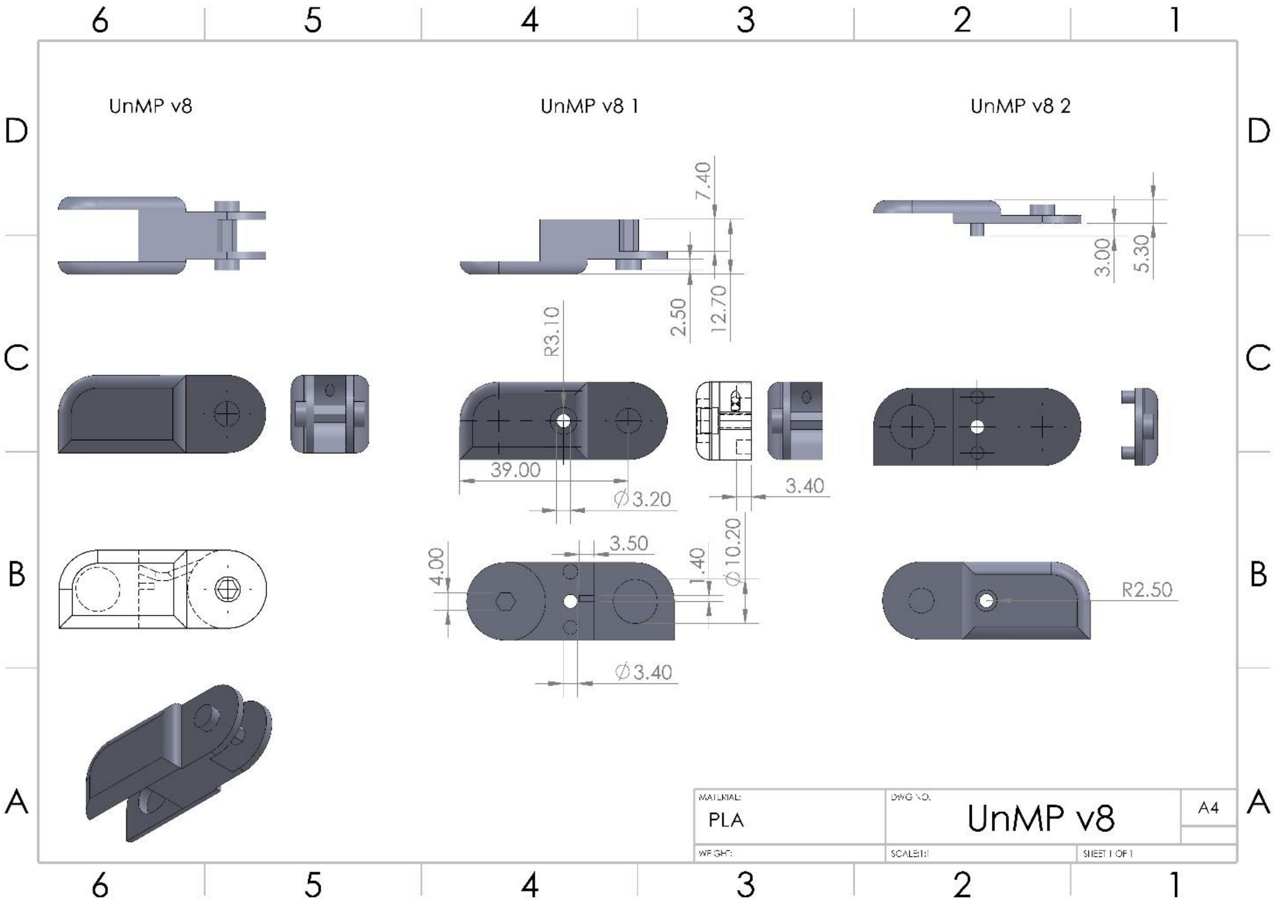

FIG 15: UnMP V8 technical drawings

The underactuated MP/PP segment of UnMP V8 was created in two printed pieces. Two identical segments were then combined for a complete underactuated finger, which resulted in fewer unique parts being produced, reduced complexity in production and provided greater flexibility when replacing damaged parts.

The underactuated MP/PP segment differs from the fully actuated phalanges because it has no tendon anchor. It features a single internal tendon channel that directs the tendon through both of the MP/PP segments so that the tendon will only anchor itself at the base of the underactuated fingertip. In addition to the internal tendon channel, each segment contains a hexagonal spring interface and a built in 90° hard stop to allow for inward flexing while preventing backward extension, similar to how our fingers naturally bend inwards in one direction.

3.12 Carpal architecture and tendon routing

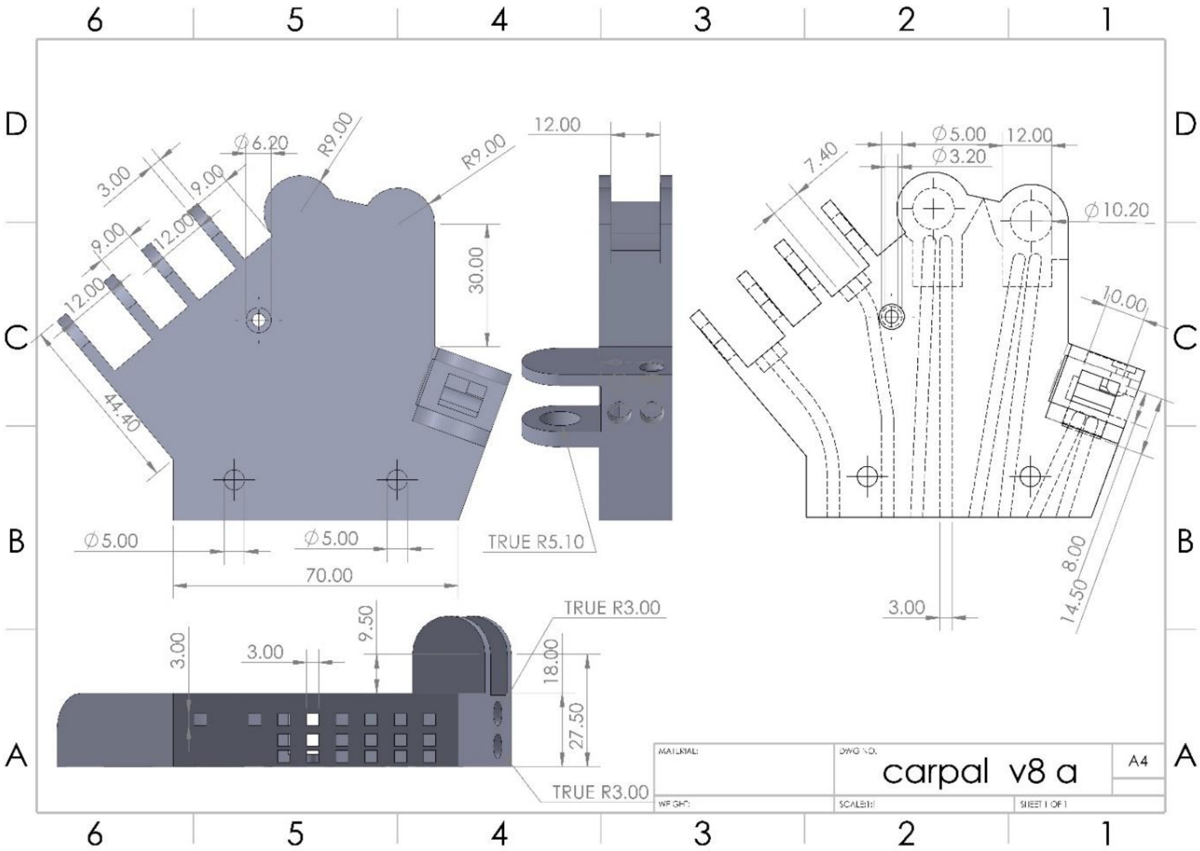

FIG 16: Carpal V8 a technical drawings

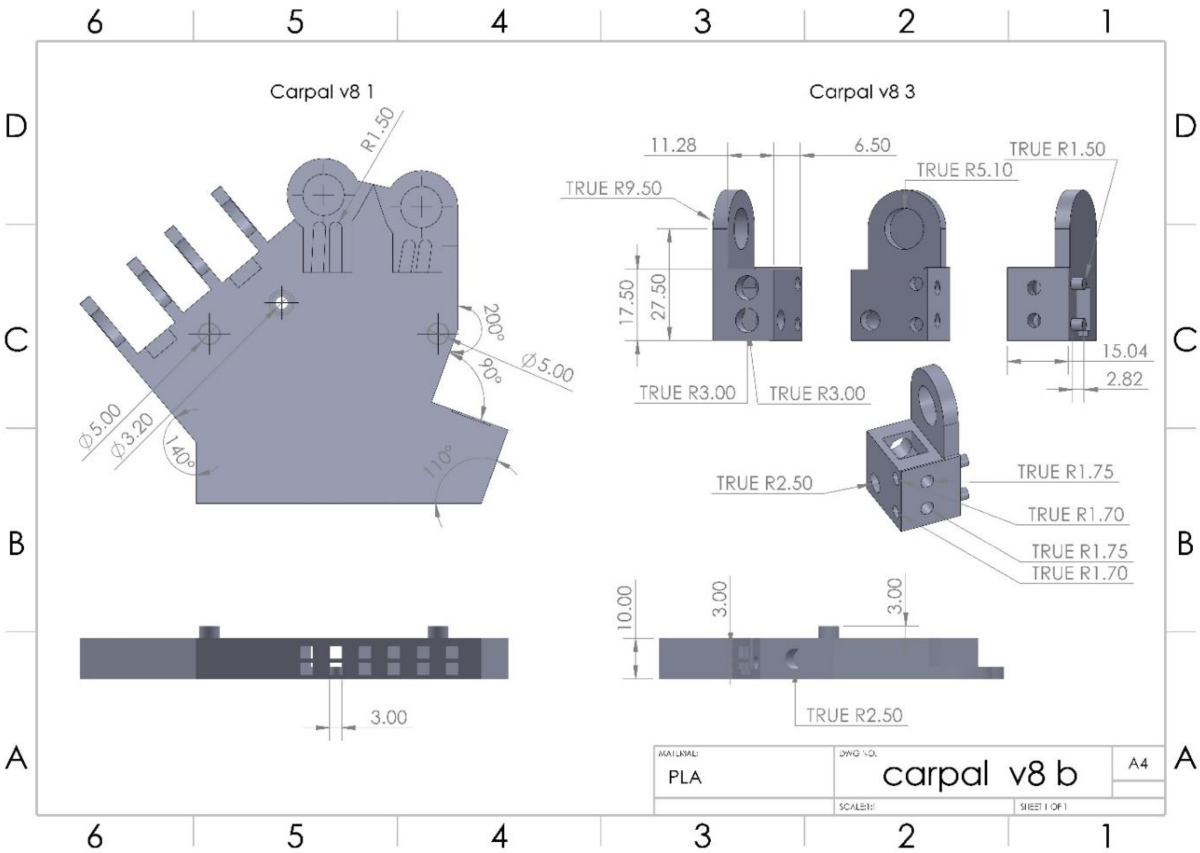

FIG 17: Carpal V8 b technical drawings

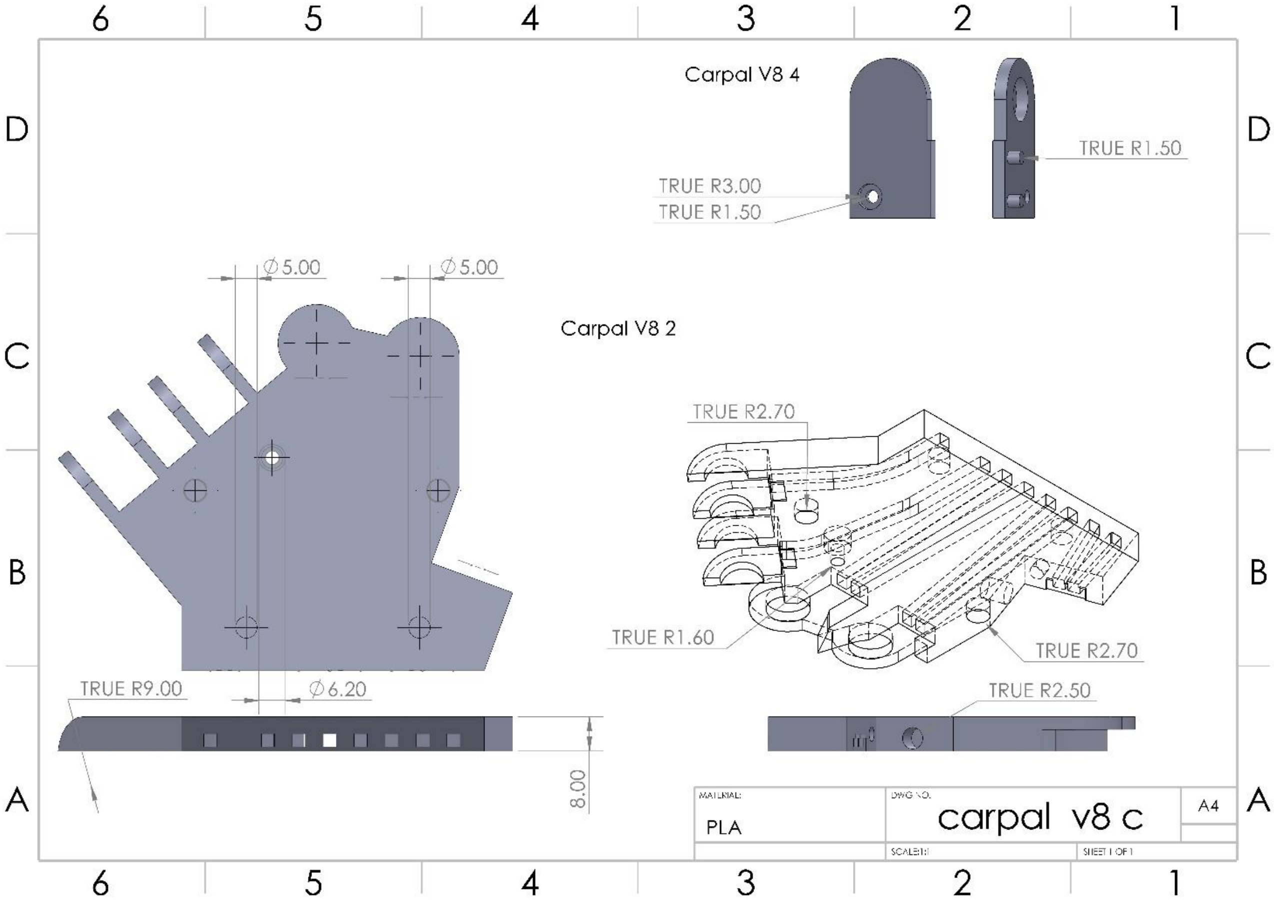

FIG 18: Carpal V8 c technical drawings

The carpal assembly was split into four printed parts to reduce print risk and allow the larger sections to be printed flat. They are made up of four printed parts in total. The lower body of the carpal is Carpal V8 1 and the upper body is Carpal V8 2. Both of these parts house the primary tendon pathways. Carpal V8 3 houses the thumb mounting bracket and Carpal V8 4 houses the opposing bearing support.

The function of the carpal was primarily for tendon organization and finger placement. There were three vertically stacked push-pull tendon sets for the fully actuated fingers: one set controlled the MP front-back motion; one set controlled the PP side to side motion; and the third set controlled the fingertip front-back motion. The thumb also routed its tendons in a manner consistent with the other fingers, however, since the joints were arranged differently than those on the fully actuated fingers, the tendon sets were rearranged to accommodate the joint arrangement of the thumb. The underactuated fingers utilized only a single tendon route that exited through the left side of Carpal V8 2. An angled slot within each finger's respective housing determined where the underactuated finger would spread to provide a more human-like design without compromising serviceability of the individual routing channels.

3.13 Motor hub

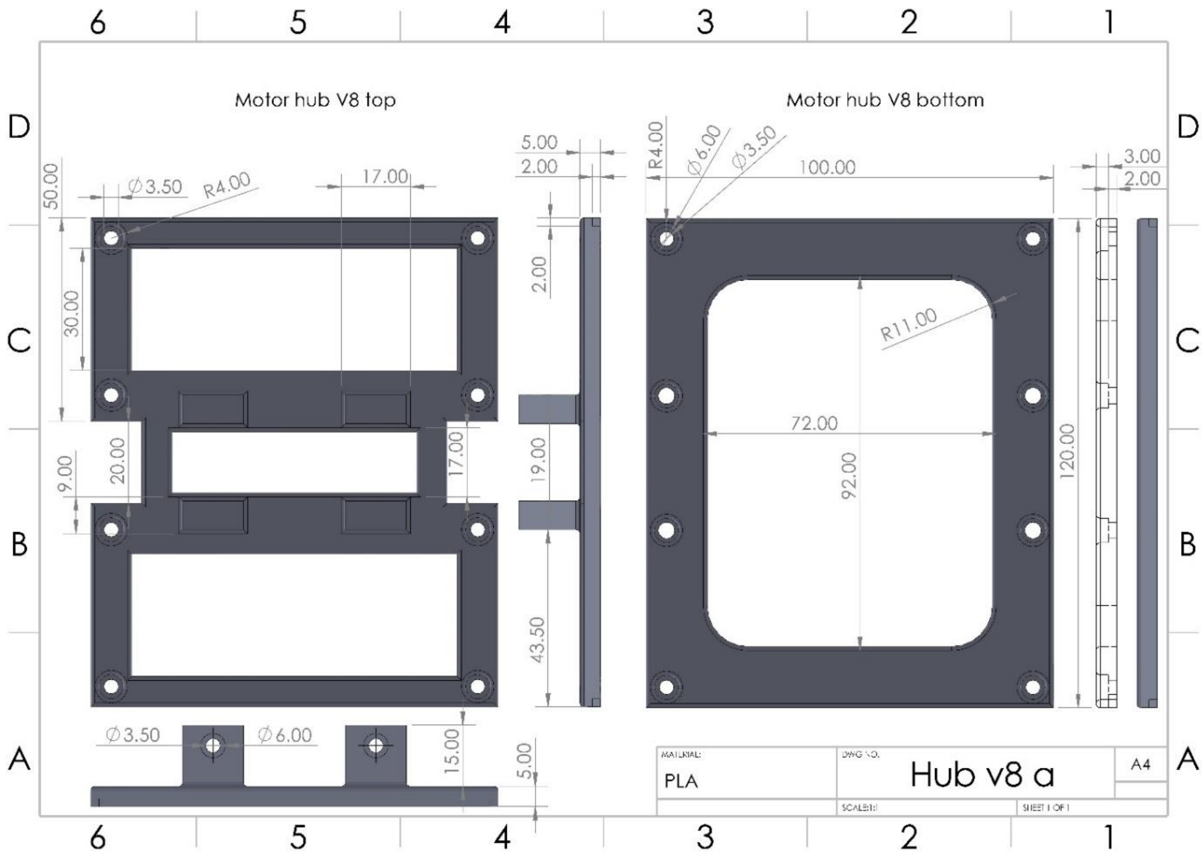

FIG 19: Hub V8 a technical drawings

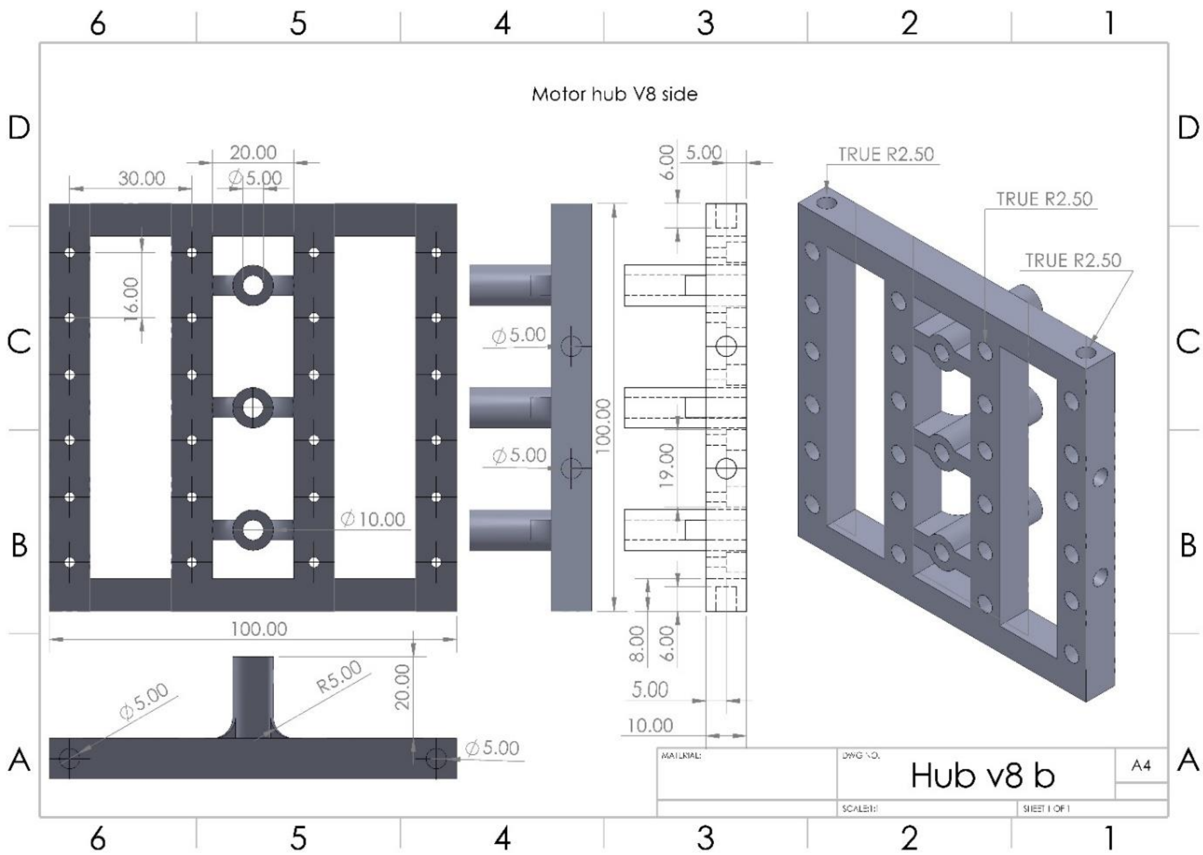

FIG 20: Hub V8 b technical drawings

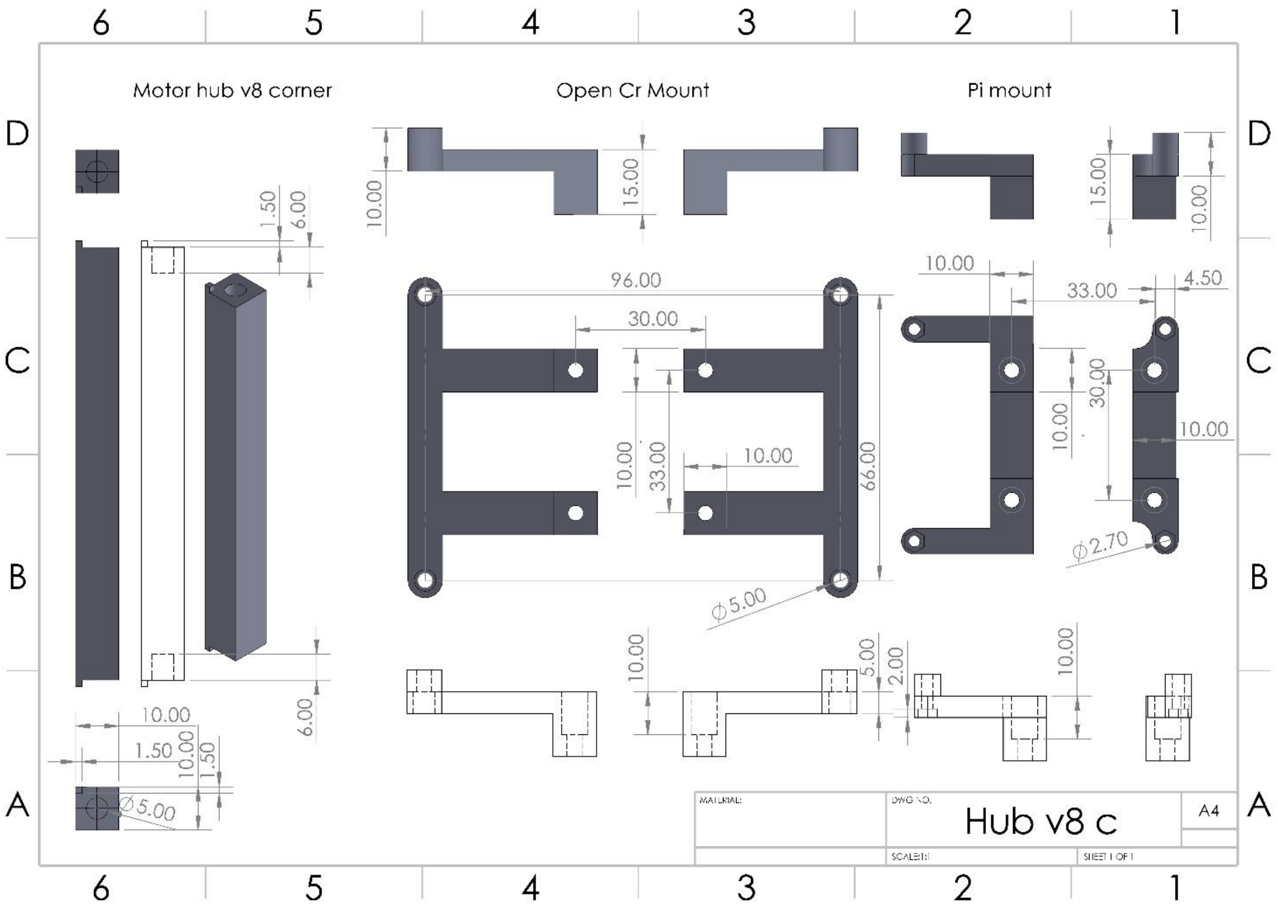

FIG 21: Hub V8 c technical drawings

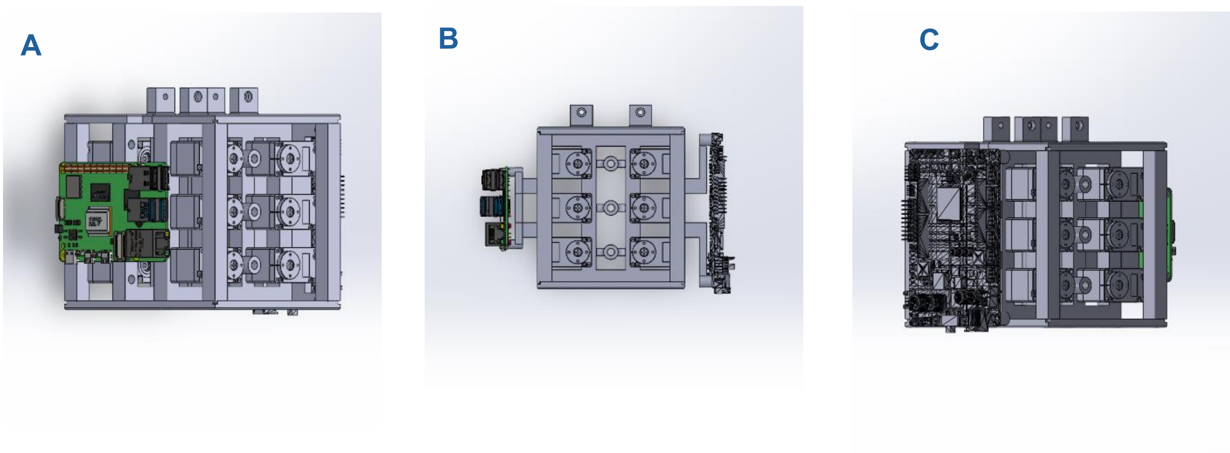

FIG 22 (A,B&C): (¾ left, front and ¾ right) view of the hub assembly

A motor hub was developed as an easily removable rear unit that utilizes Motor Hub V8 top, bottom, side and corner components. The top part of the Motor Hub is interfaced to the carpal; the bottom provides the base for the lower frame. The side parts provide mounting points for the motor arrays, and the corner parts complete the enclosure and alignment of the structure. The mounts for the OpenCR and Raspberry Pi 5 are located on the exterior face of the hub.

The size of the hub was determined for use with up to 12 DYNAMIXEL XC330-T288-T motors. Ten positions were used in the final prototype. The design of the hub allows for a compact arrangement of the motors while still maintaining accessibility to all motor faces. To reduce materials used and improve wire and assembly access rectangular openings were used throughout. For added support, multiple side hole locations were provided for screw fasteners. Tendons entered the hub from the carpal side, and due to separation via corresponding slots, they reached their respective spool holder locations prior to entering the motor. The hub was designed as a modular attachment to the hand that would allow removal of the actuator and electronic packages from the carpal/finger assembly to facilitate testing, repair or future redesign.

3.14 Tendon motor mounts

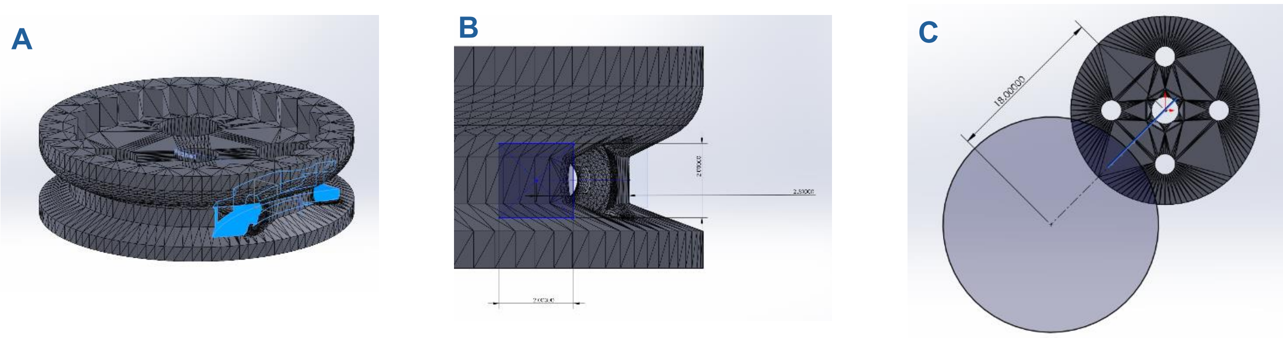

FIG 23 (A,B&C): Base spool adaptation [1]

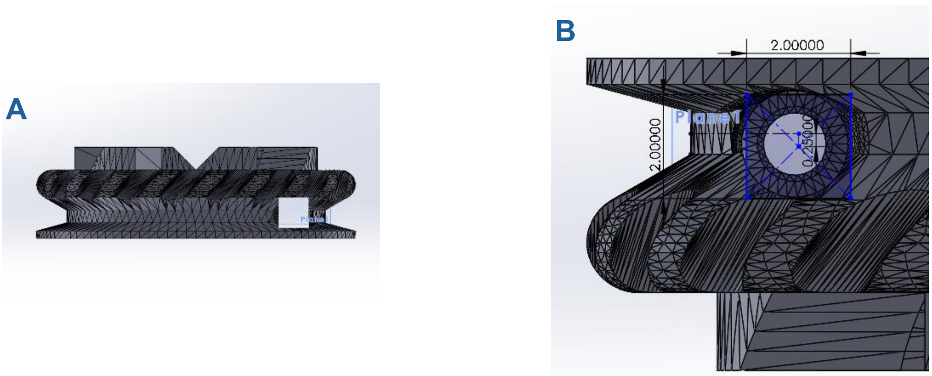

FIG 24 (A&B): Spool cover adaptation [1]

Modified ORCA STL components were reused to develop the tendon motor mounts since the original spool geometry was appropriate for wrapping around the tendon wires. As stated previously however, the imported STL geometry did not have a direct parametric relationship. Therefore, these parts were initially loaded into SolidWorks as solid bodies and then edited by using SolidWorks cut features.

The original 0.5 mm circular tendon holes were too small for the colour-coded tendon labels used during assembly. Consequently, both tendon hole sizes were increased to 1 mm x 1 mm squares. A sweep cut feature was used on the base spool and a basic cut feature was employed on the spool cover such that the original spool holder could remain intact but adapted to accommodate our project's assembly methods.

3.15 Final CAD assembly

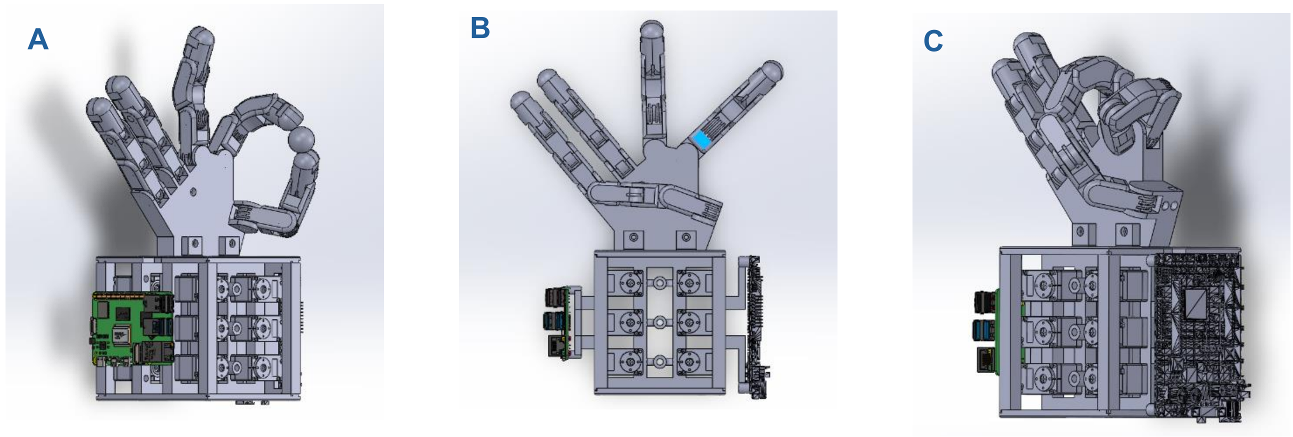

FIG 25 (A,B&C): (¾ left, front and ¾ right) view of the full V8 assembly

The final CAD assembly provided proof of concept validation of the entire architecture. Although this is neither a static force analysis nor a dynamic simulation, the CAD model demonstrated with certainty that the theoretical geometric design would be able to provide all necessary functional positions when assembled.

Representative functional positions were examined to determine if the design could demonstrate sufficient dexterity. These checks showed that finger spacing and thumb placement allowed the thumb can sufficiently oppose the index finger on an object shaped like a sphere; similarly, the thumb could move toward the base of the little finger and touch the middle fingertip. Finally, the index finger could bend toward the wrist area. These checks suggested that the current placement of the thumb, finger spacing, and limitation of the joints are sufficient to produce human-like opposition and grasping motions.

4. Results and Outcomes

4.1 Manufacturing and assembly:

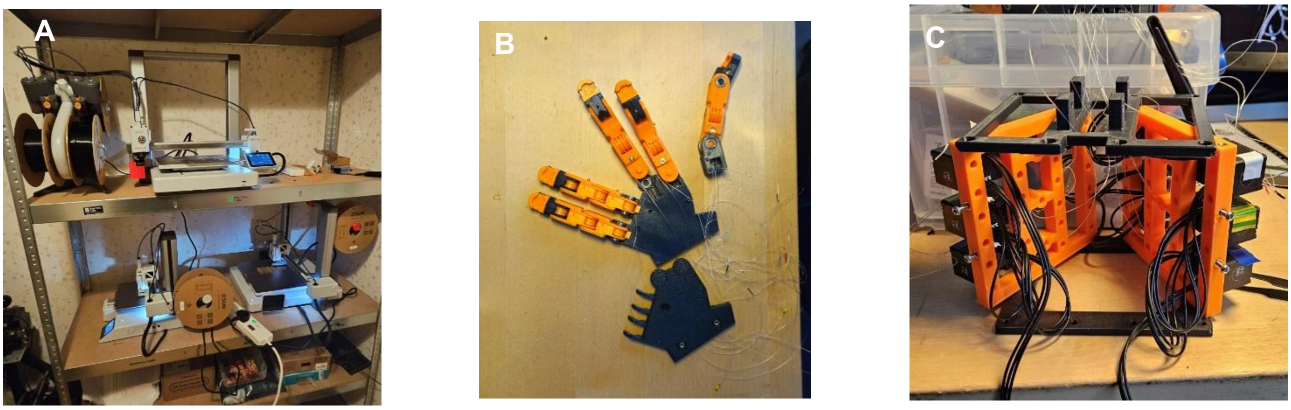

FIG 26 (A,B&C): A Printers, B prototype carpal assembly and C prototype hub assembly

The completed prototype was manufactured as an FDM printed hand assembly, with all structural elements printed in PLA [33]. Printing was completed using two Bambu Lab A1 printers and one Bambu Lab A1 Mini. Multiple sub-assemblies were built at the same time allowing for simultaneous development. The colour of each part was dependent upon available filament stock rather than function. Although PLA provided sufficient stiffness and consistent prints to create a proof of concept prototype, it should not be considered the final material choice without additional fatigue and durability tests.

Upon completion of the prints, the required inserts were installed using a soldering iron and the individual finger assemblies were combined prior to attachment to the carpal structure. The completed hand consisted of two fully-actuated fingers, two underactuated fingers and one fully-actuated thumb, demonstrating that the CAD model could be translated into a complete physical assembly rather than isolated printed parts. No major tolerance, insert-retention or alignment issues were encountered during assembly. Therefore, the clearances and split-part methodology selected appear to be suitable for production.

Tendon routing was a key assembly outcome. Electrical tape was heated and shrunk to the end of each tendon to determine joint function; i.e., black and white were assigned to the outermost push-pull pair, gray and yellow to the second joint from the top and red and blue to the last joint toward the carpal. This assisted in eliminating ambiguity in routing when there were multiple tendons going through the carpal and motor hub. Once inside the Motor Hub V8 side components, the tendons were separated based on their respective slots to prevent crossovers and assist in positioning each tendon to match its proper motor location.

All ten DYNAMIXEL XC330-T288-T [34] motors were installed and assembled with the actuation module. The modified ORCA derived spool holders were utilized to wrap and tension each tendon through their printed spring mechanism and adjustment tool. These modifications allowed for a much more precise method of tensioning each tendon compared to simply pulling each tendon tightly and securing them together. In addition, the Raspberry Pi 5 [35] and OpenCR [36] were mounted utilizing custom brackets along with being wired accordingly. As such, this validated that the mechanical packaging would support all necessary electronic components for integrated testing. However, this stage verified manufacturing feasibility and integration only; tendon efficiency, grasp force, fatigue life and repeatable control performance were not quantified.

4.2 Final prototype:

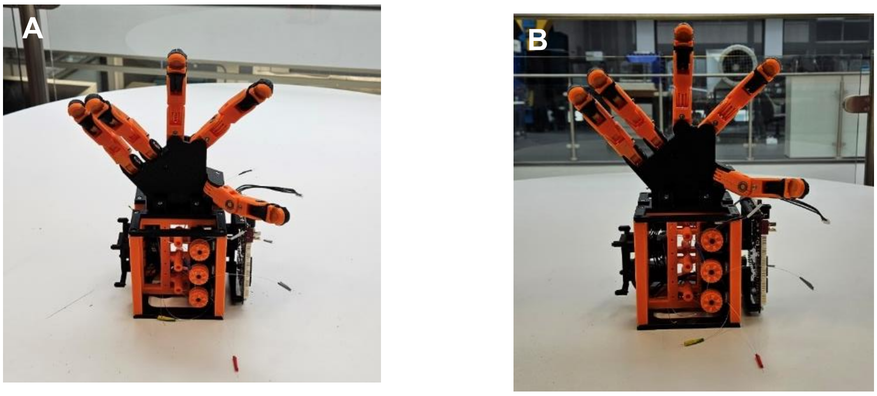

FIG 27 (A&B): prototype pre sensors

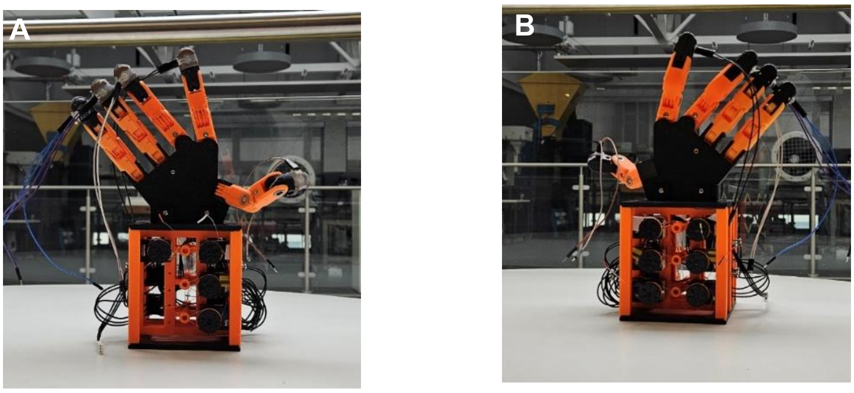

FIG 28 (A&B): Final Prototype completely assembled

Prior to completing the installation of the sensor modules onto the sensing fingertips, the first mechanically completed assembly was delivered to the electronics group for preliminary actuation and electronics testing. By delivering test versions in stages, powered movement could be initially assessed without halting progress until the sensor modules had been manufactured and calibrated.

The initial assessment conducted by the electronics group indicated that the hand moved as expected. Thus, they concluded that the tendon routing, spool configuration, and constraint imposed by each joint were effective for powered movement. Henceforth, the design progressed beyond merely validating CAD models via manual assembly inspections and was successfully transitioned from conceptual designs into actual working prototypes. Following initial testing, the prototype was returned to allow completion of installing sensing fingertips. Subsequently, after all sensing fingertips had been installed, the hand was returned to allow for comprehensive testing of both sensory responses and continued actuation.

As such, a physically constructed and integrated robotic hand capable of supporting both actuation and sensing functions as well as offering electronic capability in one system was developed. However, testing remained short term and functional rather than quantitative; repeatability, backlash, tendon friction and grasp force were not measured.

5. Analysis and Findings

5.1 CBOM Analysis

TABLE 3: CBOM

Part	Cost per pack (Inc UK VAT)	Units per Pack	Units need	Packs purchased	Total
PLA 1KG Spool	£21.50	1	1	1	£21.50
Sensors	£8.69	2	5	3	£26.07
DYNAMIXEL (XC330-T288-T)	£83.52	1	10	10	£835.20
Open CR	£203.70	1	1	1	£203.70
Raspberry Pi 5 2GB	£62.40	1	1	1	£62.40
Bearings (1063ZZ)	£7.99	10	15	2	£15.98
M3 hardware kit	£7.88	1	1	1	£7.88
M2 hardware kit	£5.29	1	1	1	£5.29
Nylon fishing line	£4.12	1	1	1	£4.12
Heated inserts M3	£5.59	1	1	1	£5.59
Electrical tape	£7.66	1	1	1	£7.66
TOTAL					£1195.39

The CBOM was produced for the complete final prototype, including printed structure, actuators, sensing elements, bearings, hardware, tendon material and main control electronics. The total prototype cost was £1195.39. This is the approximate repeat-build cost of the final design, not the total development cost, because it excludes labour, CAD time, machine use, electricity, tools, failed prints and earlier iterations.

The main finding is that cost is dominated by actuation and control hardware. The ten DYNAMIXEL XC330-T288-T motors cost £835.20 [34], approximately 69.9% of the CBOM. Including the OpenCR [36] and Raspberry Pi 5 [35] increases the motor/control subtotal to £1101.30, or about 92.1% of the total. In contrast, the printed structure and mechanical consumables were inexpensive: PLA cost £21.50, less than one 1 kg spool was used for one assembled hand, and the final FSR sensors cost £26.07.

This shows that the mechanical architecture is cost-efficient, while the total prototype cost is constrained mainly by the actuator selection. The CBOM is therefore positive for a five-digit, sensor-integrated research prototype, but it also identifies the clearest cost-reduction route: cheaper actuators combined with separate position sensing. The CBOM remains limited by supplier price changes, VAT, availability, shipping and the exclusion of institutional resources.

5.2 Analysis Against Mechanical Requirements

The Mechanical Design was assessed against the following Mechanical Requirements: FDM Manufacturability, Modularity, Tendon Driven Actuation, Integration of Sensing Mechanisms, Dexterous Motion Generation, Packaging of Electronic Components, Low Cost and Hand Over Readiness. Overall, these requirements were met at proof-of-concept level.

FDM Manufacturability and Modularity are the Strongest Outcomes. All of the final structural parts printed in PLA were assembled with no major tolerance issues, inserts or alignment problems. The split phalanx parts, removeable sensing fingertips, replaceable finger modules, separate carpal sections and detachable motor hub increased serviceability since individual components can be replaced without the need to disassemble the entire assembly.

Tendon Driven Actuation was successfully demonstrated. The tendons were routed from each finger through the carpal section into the motor hub and powered testing did show that the hand moved in the correct direction. However there are many other factors involved in Tendon Driven Actuation such as; Tendon Friction, Backlash, Repeatability and Force Transmission which have not been Quantitatively Measured. Furthermore, the spool tensioning mechanism has the possibility of loosening over a period of time if there is not some small pre-load applied to the tendons during assembly to prevent loss of tension over a period of time and ensure long term tension stability.

Integration of Sensing Mechanisms was successful from a mechanical point of view as the calibrated fingertip modules were fitted and subsequent testing confirmed that the sensing mechanisms responded correctly during actuated operation.

Dexterity motion was demonstrated in CAD renderings such as Thumb Index Opposition, Thumb Reach Towards Little Finger Base, Thumb Middle Contact and Index Flexion Towards Carpal Section. Therefore although this demonstrates motion capability rather than manipulation performance the design fulfils all the principal mechanical requirements except for: Durability, Fatigue Grasp Force and Long Cycle Reliability which require further Quantitative Testing.

6. Discussion of Findings, Evaluation and Implications

6.1 Critical Evaluation of the Final Design

The final design was successful as a mechanical proof-of-concept because it delivered a complete, manufacturable and integrated robotic hand rather than only a CAD model. Moving away from direct ORCA adaptation increased the design workload, but it also gave greater control over geometry, tolerances, tendon routing, sensor access and assembly. This was necessary because the imported ORCA files could not be reliably modified parametrically.

One of the most significant strengths of the final design was its modularity. With split-phalanx components, removable sensing fingertips, a separable carpal module and a removable motor-hub, the hand could be built and serviced in sections. This approach minimized the possibility that a localized failure such as wear on a tendon path or insertion point of sensors would require reprinting of a major portion of the hand. The removable fingertip sensing units were particularly beneficial since they provided the ability to manufacture, calibrate and replace sensing units without having to remove entire fingers.

The tendon system functioned well at the prototype stage; with all tendons properly routed throughout the fingers, carpal and motor hub. In addition, during power-up testing, motion occurred in the direction that was expected. Despite these accomplishments however, this represents one of the primary technical limitations of the design. None of the effects related to friction generated by the tendons (backlash), potential long term slacking of tendons due to flexural deformation and/or creep relaxation, repeatibility of positioning/forces developed when grasping objects and overall grasp forces have been measured. As such, the design cannot currently be said to be performance verified. An additional weak area of the reused ORCA derived spool-tensioning mechanism is that it will lose tension over time if no slight pre-tension is maintained on the tendons.

As a whole, the design has fulfilled the requirements of the mechanical aspects of manufacturability, modularity, tendon-actuated, accommodating sensing and integrating into other systems. Its greatest value is likely to be as a research ready prototype platform. Additional verification of the design will need to occur through testing of grip-forces, fatigue testing of the hand/tendons, measurements of efficiency of tendon movement and multiple repetitions of actuating motions.

6.2 Health, safety, ethics, sustainability, and standards

Health, safety, ethics and sustainability considerations were important since the prototype included; moving joints, tendons, motor spools, heat-set inserts and embedded electronic components. The Engineering Council's ethical principles and Institute of Mechanical Engineers' (IMechE) Code of Conduct both state that the project must be reported truthfully and fairly without exaggeration of the prototypes performance [37], [38]. Therefore, the report states some limitations to the prototype including; unmeasured force, fatigue-life, backlash and short term PLA durability.

The primary safety concerns in the prototype include: pinch points from the mechanical arms/tendons, tendon snap back when they move too far; rotating spool which can catch clothing or loose hair; exposed wiring and burn risk from insertion of heat set inserts. As stated above these hazards have been mitigated through careful assembly with stoppers on the moving parts and for longer assemblies; through modular design and testing, however further development will need to include guard rails, emergency stopping behavior, electrical protection before longer term demonstrations are performed.

PLA , has many sustainable benefits including being made from renewable resources and also biodegradable and recyclable/compostable provided that disposal is done properly. However, it does not provide environmental neutrality. The reusable DYNAMIXEL motors and replaceable printed modules help to limit waste generated by the development of future versions. Standards Compliance is limited since this is a prototype designed in academia rather than a commercially available product.

7. Conclusion

A whole mechanical design, manufactured prototype and integrated hardware platform for the Dextrous Robotic Hand with Multimodal Sensing has been completed in this project. It had originally intended to modify the open-source ORCA hand [1] . However, due to the unreliability of parametric modifications based on the provided CAD files, the necessary levels of sensing, actuation and packaging integration could not be achieved. Therefore, the mechanical work package went from adapting the open source ORCA hand to a completely new original design while still maintaining all of the goals of creating a low-cost, modular, tendon-driven and sensor compatible robotic hand.

As such, the end result was a functional prototype of a five-fingered robotic hand (two fully active fingers, two underactive fingers and one active thumb). This consisted of a series of split-phalanx assemblies, tendon anchors, organized carpal routing, removable sensing fingertips; an integrated motor hub; and mounting locations for both the Raspberry Pi 5 and OpenCR. The prototype was printed using PLA, assembled with bearings, heat set inserts and fasteners, and then passed off to be tested for electronics and actuation. Testing showed actuation in the expected directions, as well as confirmed that the sensing fingertips can be mounted without impeding finger motion during later integration.

The major contribution of this project is showing that the final CAD architecture for the robotic hand was capable of being manufactured at a physical scale, assembled into its various components, and integrated as separate subsystems. The modularity of the design made it easier to repair/replace individual modules rather than having to reprint entire sections of the robot if something fails or needs to be updated. The CBOM also illustrated that the cost of printing the mechanical structure was relatively low compared to other parts of the overall robotic hand system.

While the prototype represents a proof-of-concept rather than a fully validated robotic hand, initial testing did show that functional feasibility existed. As stated earlier however, there are several additional issues that need to be addressed prior to the creation of a functional, commercially viable product: grasp force, tendon friction, backlash, fatigue life, repeatability and long-term use of the PLA material.

8. Future Work

8.1 Immediate next steps

Immediate priority will be to complete a structural mechanical testing program to identify weak points in the mechanical structure of the prototype. During initial tests using manual assembly, activation was successful for short periods. There has been no test of behavior with repeated loads, increased tendon tension, and longer duration of operation. Thus, all joints are to be tested to failure or observable degradation, and the location and type of each failure are to be documented. Testing is to focus on tendon anchor points (slip), printed spring elements (loss of stiffness, cracking or permanent deformation), heat set inserts (retention due to surrounding printed material), and the spool tensioning system.

Testing should specifically check for anchor slip, knot pull-through at anchor points, and cracking around recessed pocket areas. Loss of stiffness, cracking, and/or permanent deformation of the underactuated spring members are to be determined as well as inspection for retention of inserts after multiple assemblies and loadings since retention is dependent upon surrounding printed material. Performance measurements are to be taken instead of relying solely upon visual assessments. Range of motion, repeatability, backlash, tendon slippage, grip force, and frictional losses through the carpal and motor hubs are to be evaluated.

Additionally, the spool tensioning mechanism needs to be redesigned since it currently lacks an ability to positively lock or independently adjust tension prior to engaging slight tendon pre-tension which significantly improves reliability.

8.2 Further work

Long-term work should reduce the actuator cost while maintaining controllability. The costed bill of materials showed that the DYNAMIXEL motors accounted for a significant majority of the total cost; therefore, consideration should be given to low-cost actuators. However, if smart servo motors are replaced with less expensive alternatives, it is likely that the use of some of the built in feedback will also be reduced. Therefore, an alternative approach may be to provide dedicated joint position sensing as part of the mechanical design.

9. Project Gantt Chart

TABLE 4: Project Gantt Chart

Task		Allocation	Start	Finish	Phase	22/09/2025	29/09/2025	06/10/2025	13/10/2025	20/10/2025	27/10/2025	03/11/2025	10/11/2025	17/11/2025	24/11/2025	01/12/2025	08/12/2025	15/12/2025	22/12/2025	29/12/2025	05/01/2026	12/01/2026	19/01/2026	26/01/2026	02/02/2026	09/02/2026	16/02/2026	23/02/2026	02/03/2026	09/03/2026	16/03/2026	23/03/2026	30/03/2026	06/04/2026	13/04/2026	20/04/2026
1	Project initiation and team setup	Team	23.9.25	9.10.25	Initiation																															
2	Background research and ORCA review	Team	26.9.25	21.10.25	Research																															
3	Requirements, motor count and CBOM	Team	14.10.25	31.10.25	Planning																															
4	V1–V2 CAD concept development	Shannen	28.10.25	17.12.25	CAD design																															
5	CW1 RAO presentation	Team	13.11.25	8.12.25	Assessment																															
6	V3 tendon routing CAD	Shannen	28.11.25	15.1.26	CAD design																															
7	Sensor tip geometry and mould design	Shannen & Sensors	15.12.25	4.2.26	Sensor integration																															
8	Hardware ordering and preparation	Team	18.12.25	27.3.26	Procurement																															
9	V4 CAD, print and single-finger testing	Shannen & Electronics	22.1.26	13.2.26	Prototype testing																															
10	CW2 / ILF preparation and demonstration	Team	17.2.26	11.3.26	Assessment																															
11	V5 underactuation and thumb feedback	Shannen & Team	23.2.26	27.2.26	Design feedback																															
12	V7 full assembly and motor hub	Shannen	6.3.26	23.3.26	Assembly																															
13	Post-handover improvements and V7 testing	Shannen & Electronics	24.3.26	6.4.26	Testing/improvement																															
14	V8 carpal redesign and final routing	Shannen	7.4.26	13.4.26	Final redesign																															
15	Final actuation handover	Shannen & Electronics	14.4.26	16.4.26	Handover																															
16	Sensor fingertip integration	Shannen & Sensors	17.4.26	21.4.26	Final integration																															
Milestones									●								●									●				●			●		●	●

10. References

[1] C. C. Christoph *et al.*, ‘ORCA: An Open-Source, Reliable, Cost-Effective, Anthropomorphic Robotic Hand for Uninterrupted Dexterous Task Learning’, in *2025 IEEE/RSJ International Conference on Intelligent Robots and Systems (IROS)*, Hangzhou, China: IEEE, Oct. 2025, pp. 8503–8510. doi: 10.1109/IROS60139.2025.11246681.

[2] C. Piazza, G. Grioli, M. G. Catalano, and A. Bicchi, ‘A Century of Robotic Hands’, *Annu. Rev. Control Robot. Auton. Syst.*, vol. 2, no. 1, pp. 1–32, May 2019, doi: 10.1146/annurev-control-060117-105003.

[3] A. Saudabayev and H. A. Varol, ‘Sensors for Robotic Hands: A Survey of State of the Art’, *IEEE Access*, vol. 3, pp. 1765–1782, 2015, doi: 10.1109/ACCESS.2015.2482543.

[4] M. Baggetta, A. Rittore, and G. Berselli, ‘On the Modeling of Tendon-Driven Systems: a Literature Review’, in *2024 20th IEEE/ASME International Conference on Mechatronic and Embedded Systems and Applications (MESA)*, Genova, Italy: IEEE, Sep. 2024, pp. 1–7. doi: 10.1109/MESA61532.2024.10704873.

[5] A. G. Zisimatos, M. V. Liarokapis, C. I. Mavrogiannis, and K. J. Kyriakopoulos, ‘Open-source, affordable, modular, light-weight, underactuated robot hands’, in *2014 IEEE/RSJ International Conference on Intelligent Robots and Systems*, Chicago, IL, USA: IEEE, Sep. 2014, pp. 3207–3212. doi: 10.1109/IROS.2014.6943007.

[6] T. Laliberté and C. M. Gosselin, ‘Simulation and design of underactuated mechanical hands’, *Mechanism and Machine Theory*, vol. 33, no. 1–2, pp. 39–57, Jan. 1998, doi: 10.1016/S0094-114X(97)00020-7.

[7] H. Park and D. Kim, ‘An open-source anthropomorphic robot hand system: HRI hand’, *HardwareX*, vol. 7, p. e00100, Apr. 2020, doi: 10.1016/j.ohx.2020.e00100.

[8] ‘Whimsical — Where great ideas take shape’. [Online]. Available: https://whimsical.com/

[9] A. Nurpeissova, T. Tursynbekov, and A. Shintemirov, ‘An Open-Source Mechanical Design of ALARIS Hand: A 6-DOF Anthropomorphic Robotic Hand’, in *2021 IEEE International Conference on Robotics and Automation (ICRA)*, Xi’an, China: IEEE, May 2021, pp. 1177–1183. doi: 10.1109/ICRA48506.2021.9561977.

[10] A. Bulgarelli, G. Toscana, L. O. Russo, G. A. Farulla, M. Indaco, and B. Bona, ‘A Low-Cost Open Source 3D-Printable Dexterous Anthropomorphic Robotic Hand with a Parallel Spherical Joint Wrist for Sign Languages Reproduction’, *International Journal of Advanced Robotic Systems*, vol. 13, no. 3, p. 126, May 2016, doi: 10.5772/64113.

[11] B. He, S. Wang, and Y. Liu, ‘Underactuated robotics: A review’, *International Journal of Advanced Robotic Systems*, vol. 16, no. 4, p. 1729881419862164, Jul. 2019, doi: 10.1177/1729881419862164.

[12] T. Laliberte, L. Birglen, and C. M. Gosselin, ‘Underactuation in robotic grasping hands’.

[13] E. Difonzo, G. Zappatore, G. Mantriota, and G. Reina, ‘Advances in Finger and Partial Hand Prosthetic Mechanisms’, *Robotics*, vol. 9, no. 4, p. 80, Oct. 2020, doi: 10.3390/robotics9040080.

[14] G. P. Kontoudis, M. V. Liarokapis, A. G. Zisimatos, C. I. Mavrogiannis, and K. J. Kyriakopoulos, ‘Open-source, anthropomorphic, underactuated robot hands with a selectively lockable differential mechanism: Towards affordable prostheses’, in *2015 IEEE/RSJ International Conference on Intelligent Robots and Systems (IROS)*, Hamburg, Germany: IEEE, Sep. 2015, pp. 5857–5862. doi: 10.1109/IROS.2015.7354209.

[15] S. Shirafuji, S. Ikemoto, and K. Hosoda, ‘Development of a tendon-driven robotic finger for an anthropomorphic robotic hand’, *The International Journal of Robotics Research*, vol. 33, no. 5, pp. 677–693, Apr. 2014, doi: 10.1177/0278364913518357.

[16] H. Sang, C. Yang, F. Liu, J. Yun, and F. Chen, ‘Kinematics Rapid Modeling Method of Tendon-Driven Robotic Mechanisms Using the Tendon-Routing Matrix and Equivalent Radius Matrix’,

in *Proceedings of the 2016 International Conference on Electrical, Mechanical and Industrial Engineering*, Phuket, Thailand: Atlantis Press, 2016. doi: 10.2991/icemie-16.2016.73.

[17] L. Wen, Y. Li, M. Cong, H. Lang, and Y. Du, ‘Design and optimization of a tendon-driven robotic hand’, in *2017 IEEE International Conference on Industrial Technology (ICIT)*, Toronto, ON: IEEE, Mar. 2017, pp. 767–772. doi: 10.1109/ICIT.2017.7915456.

[18] V. K. Nanayakkara, G. Cotugno, N. Vitzilaios, D. Venetsanos, T. Nanayakkara, and M. N. Sahinkaya, ‘The Role of Morphology of the Thumb in Anthropomorphic Grasping: A Review’, *Front. Mech. Eng.*, vol. 3, p. 5, Jun. 2017, doi: 10.3389/fmech.2017.00005.

[19] S. R. Kashef, S. Amini, and A. Akbarzadeh, ‘Robotic hand: A review on linkage-driven finger mechanisms of prosthetic hands and evaluation of the performance criteria’, *Mechanism and Machine Theory*, vol. 145, p. 103677, Mar. 2020, doi: 10.1016/j.mechmachtheory.2019.103677.

[20] Sung-Yoon Jung, Sung-kyun Kang, Myoung-Jun Lee, and Inhyuk Moon, ‘Design of robotic hand with tendon-driven three fingers’, in *2007 International Conference on Control, Automation and Systems*, Seoul, South Korea: IEEE, 2007, pp. 83–86. doi: 10.1109/ICCAS.2007.4406884.

[21] J. Park, M. Chang, I. Jung, H. Lee, and K. Cho, ‘3D Printing in the Design and Fabrication of Anthropomorphic Hands: A Review’, *Advanced Intelligent Systems*, vol. 6, no. 5, p. 2300607, May 2024, doi: 10.1002/aisy.202300607.

[22] H. Moeinnia, H. Su, and W. S. Kim, ‘Novel Grasping Mechanisms of 3D-Printed Prosthetic Hands’, *Advanced Intelligent Systems*, vol. 4, no. 11, p. 2200189, Nov. 2022, doi: 10.1002/aisy.202200189.

[23] J. Ten Kate, G. Smit, and P. Breedveld, ‘3D-printed upper limb prostheses: a review’, *Disability and Rehabilitation: Assistive Technology*, vol. 12, no. 3, pp. 300–314, Apr. 2017, doi: 10.1080/17483107.2016.1253117.

[24] A. Mohammadi *et al.*, ‘A practical 3D-printed soft robotic prosthetic hand with multi-articulating capabilities’, *PLoS ONE*, vol. 15, no. 5, p. e0232766, May 2020, doi: 10.1371/journal.pone.0232766.

[25] C. Porthouse, ‘Determination of Safe Tensile Loading Values fro Threaded Heat-Set Inserts’.

[26] U. Scarcia, G. Berselli, and C. Melchiorri, *Optimal design of 3D printed spiral torsion springs*, vol. 50497, V002T03A020 vols. 2016.

[27] H. Höppner, A. Kirner, J. Göttlich, L. Jakob, A. Dietrich, and C. Ott, ‘Variable Stiffness Actuation via 3D-Printed Nonlinear Torsional Springs’, *IEEE Robot. Autom. Lett.*, vol. 10, no. 5, pp. 4324–4331, May 2025, doi: 10.1109/LRA.2025.3549658.

[28] L. He, H. Peng, M. Lin, R. Konjeti, F. Guimbretière, and J. E. Froehlich, ‘Ondulé: Designing and Controlling 3D Printable Springs’, in *Proceedings of the 32nd Annual ACM Symposium on User Interface Software and Technology*, New Orleans LA USA: ACM, Oct. 2019, pp. 739–750. doi: 10.1145/3332165.3347951.

[29] B. Choi, S. Lee, H. Choi, and S. Kang, ‘Development of Anthropomorphic Robot Hand with Tactile Sensor : SKKU Hand II’, in *2006 IEEE/RSJ International Conference on Intelligent Robots and Systems*, Beijing, China: IEEE, Oct. 2006, pp. 3779–3784. doi: 10.1109/IROS.2006.281763.

[30] M. N. Saadatzi, J. R. Baptist, Z. Yang, and D. O. Popa, ‘Modeling and Fabrication of Scalable Tactile Sensor Arrays for Flexible Robot Skins’, *IEEE Sensors J.*, vol. 19, no. 17, pp. 7632–7643, Sep. 2019, doi: 10.1109/JSEN.2019.2915362.

[31] N. Fiedler, P. Ruppel, Y. Jonetzko, N. Hendrich, and J. Zhang, ‘A Low-Cost Modular System of Customizable, Versatile, and Flexible Tactile Sensor Arrays’, in *2021 IEEE/RSJ International Conference on Intelligent Robots and Systems (IROS)*, Prague, Czech Republic: IEEE, Sep. 2021, pp. 1771–1777. doi: 10.1109/IROS51168.2021.9635851.

[32] Dassault Systèmes, *SOLIDWORKS 2025*. (2025). Dassault Systèmes. [Online]. Available: https://www.solidworks.com/
[33] Bambu Lab, *Bambu Studio*. (2026). [Online]. Available: https://bambulab.com/en-gb/download/studio
[34] 'Robotis - Dynamixel XC330-T288-T'. [Online]. Available: https://robotis.co.uk/robotis-dynamixel-xc330-t288-t.html
[35] 'Raspberry Pi 5', The Pi Hut. [Online]. Available: https://thepihut.com/products/raspberry-pi-5
[36] 'OpenCR1.0'. [Online]. Available: https://robotis.co.uk/opencr1-0.html
[37] 'Guidance on ethical practices'. [Online]. Available: https://www.engc.org.uk/resources-and-guidance/guidance-for-the-profession/ethical-principles/
[38] 'Code of Conduct explained - IMechE'. [Online]. Available: https://www.imeche.org/about-us/imeche-governance/governance-and-finance-reviews/code-of-conduct-explained

11. Appendices

11.1 Tendon anchor

V1:

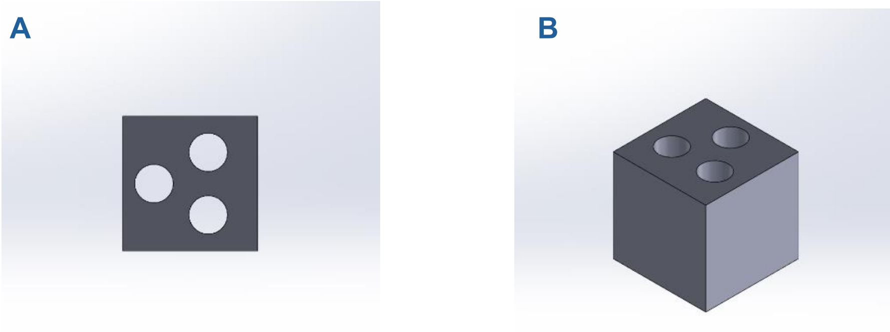

FIG 29(A&B): V1 Tendon anchor

V2:

FIG 30 (A,B&C): V2 Tendon anchor

V3:

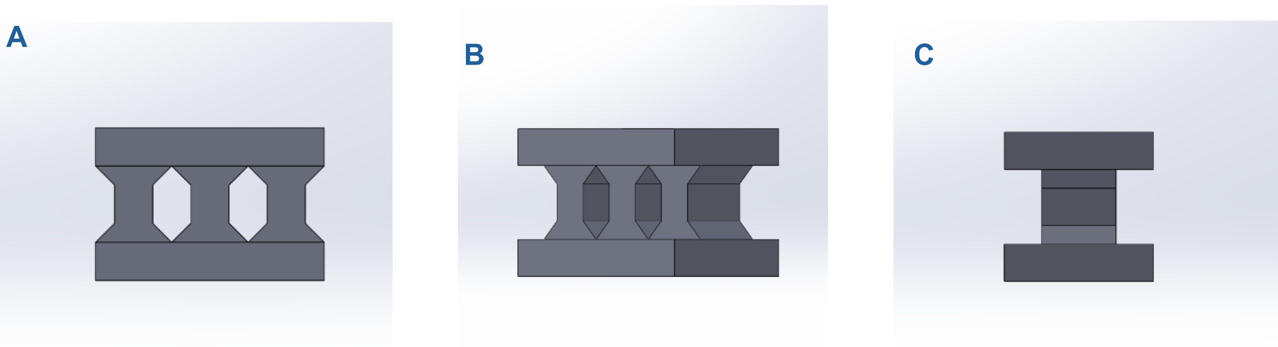

FIG 31 (A,B&C): V3 Tendon anchor

11.2 Fingertip design (DP)

V1:

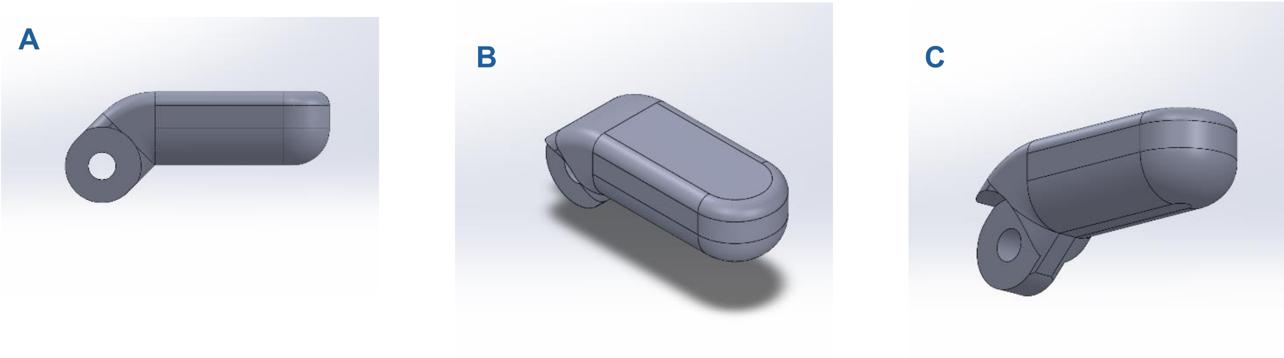

FIG 32 (A,B&C): V1 DP

V2:

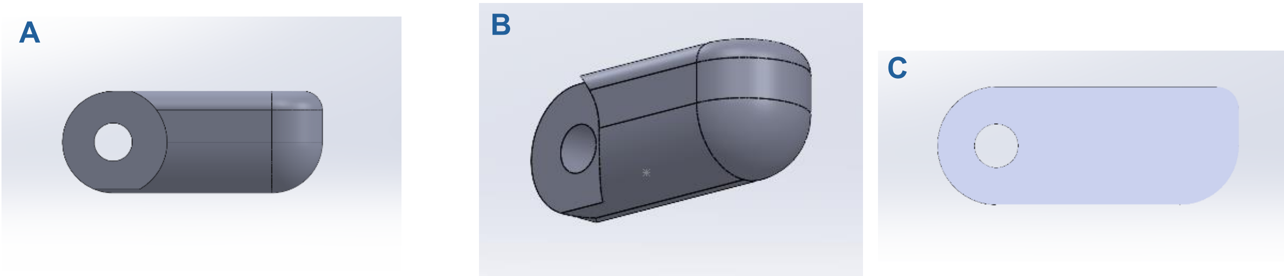

FIG 33 (A,B&C): V2 DP

V3:

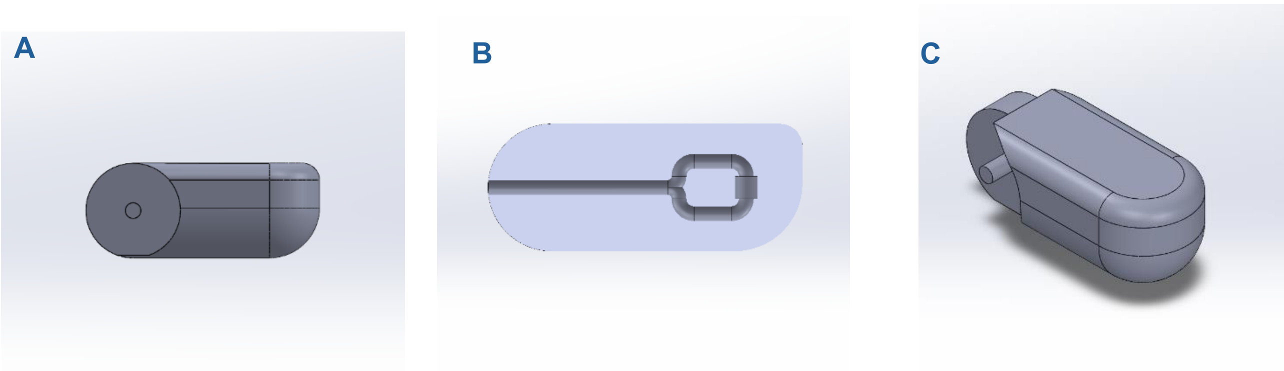

FIG 34 (A,B&C): V3 DP

V4:

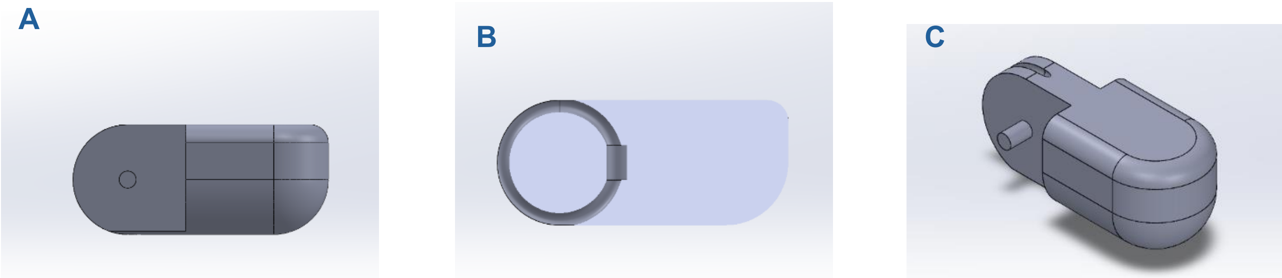

FIG 35 (A,B&C): V4 DP

V5:

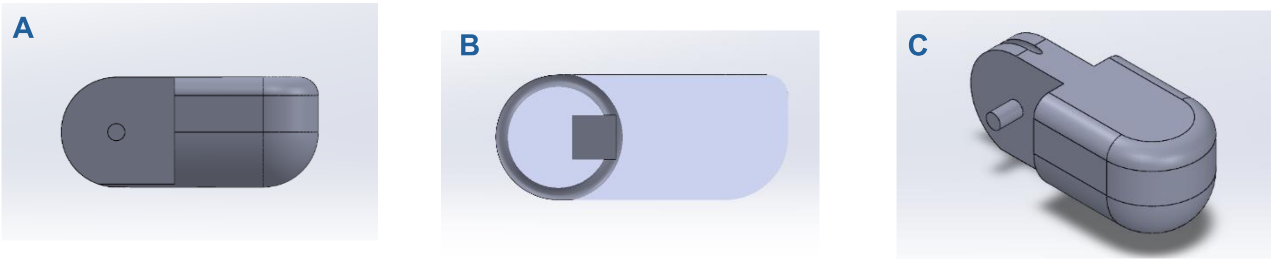

FIG 36 (A,B&C): V5 DP

V6:

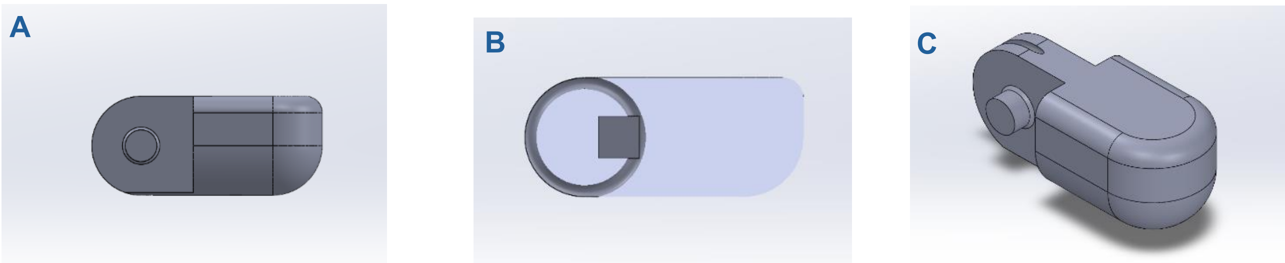

FIG 37 (A,B&C): V6 DP

V7:

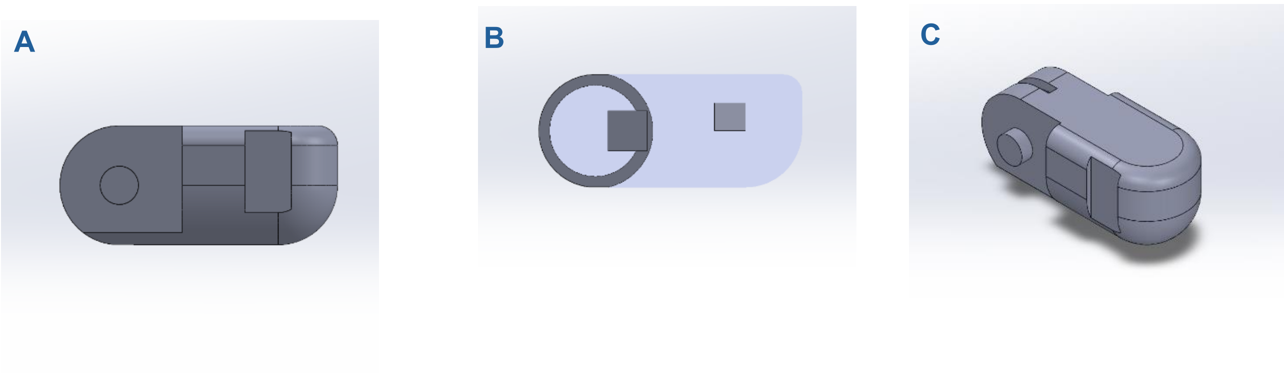

FIG 38 (A,B&C): V7 DP

11.3 Middle Phalanx Design (MP)

V1:

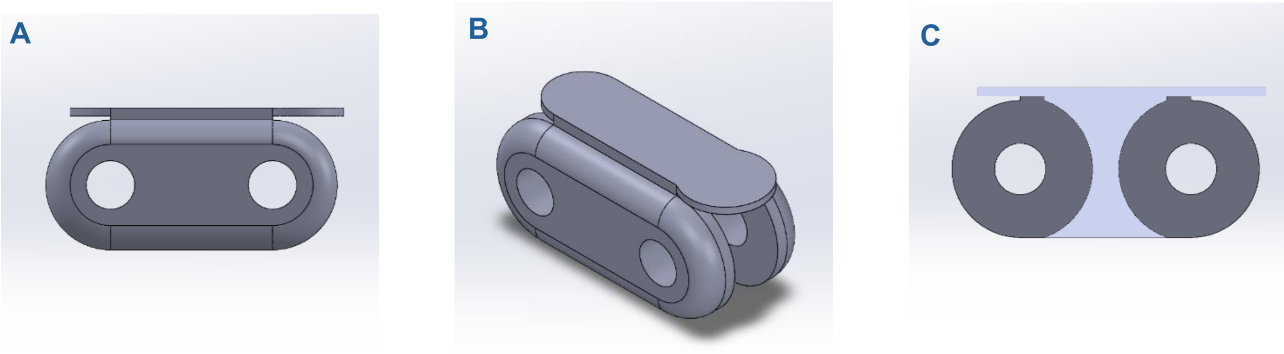

FIG 39 (A,B&C): V1 MP

V3:

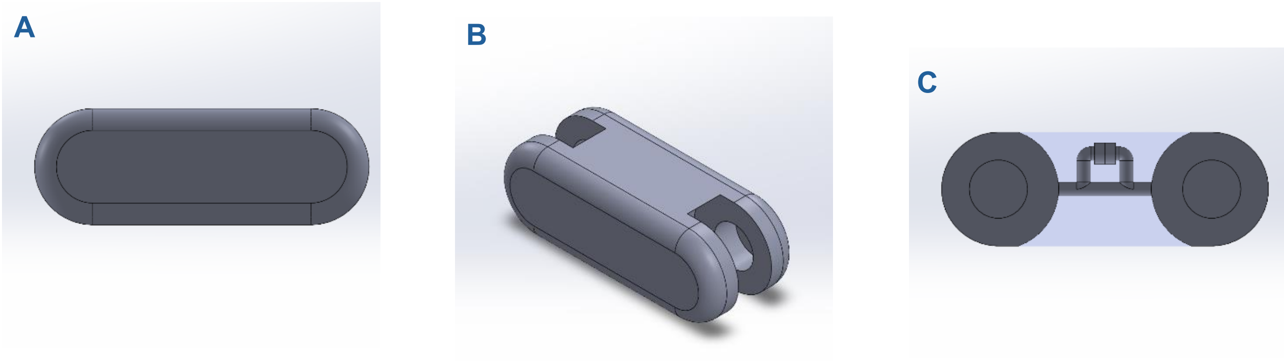

FIG 40 (A,B&C): V3 MP

V4:

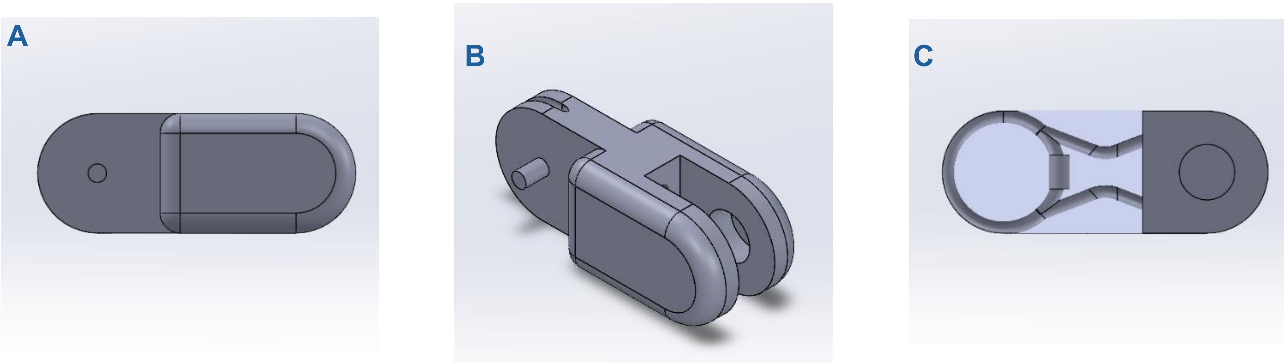

FIG 41 (A,B&C): V4 MP

V5:

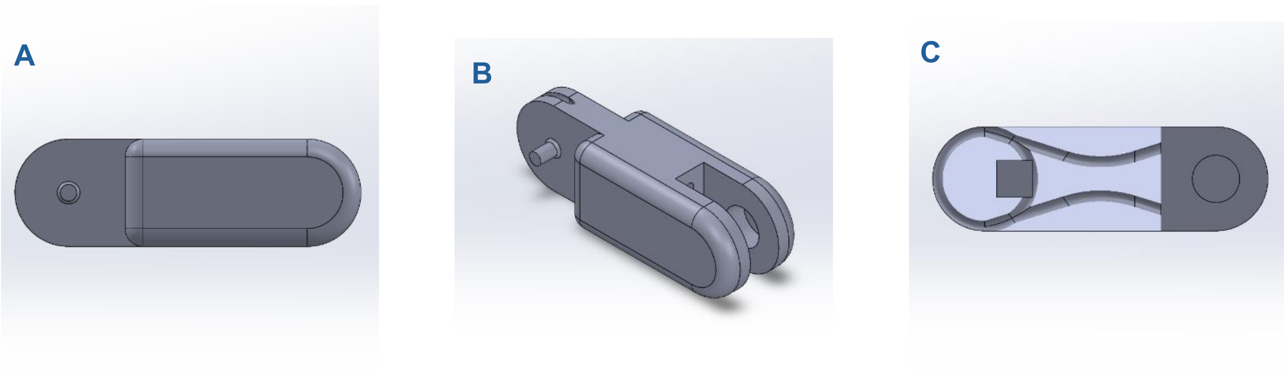

FIG 42 (A,B&C): V5 MP

V7:

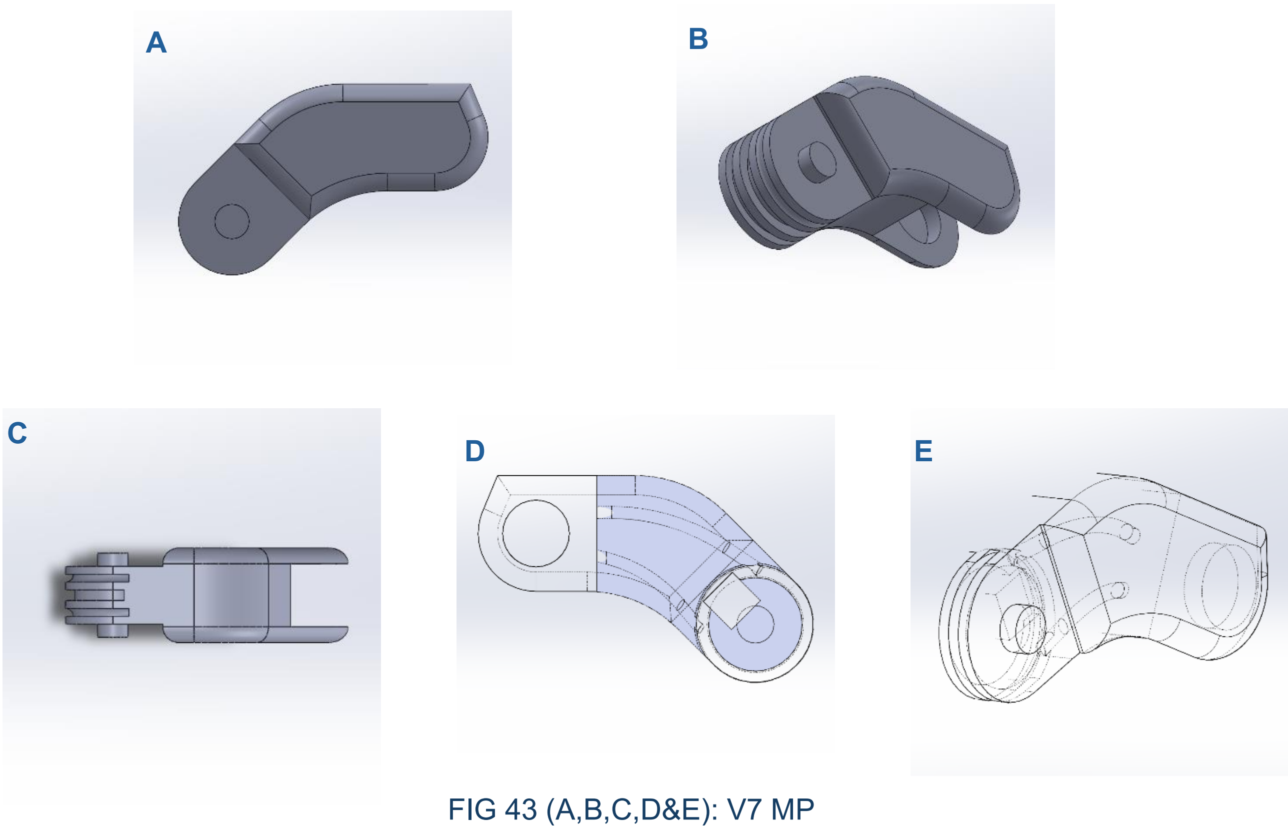

FIG 43 (A,B,C,D&E): V7 MP

11.4 Proximal/end segment design (PP)

V1:

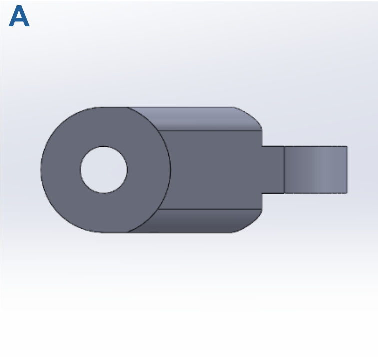

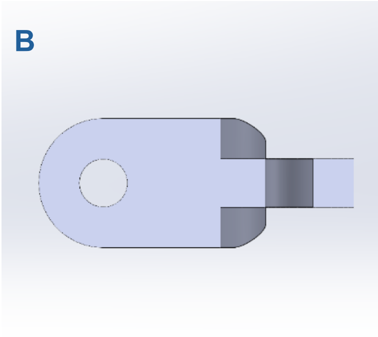

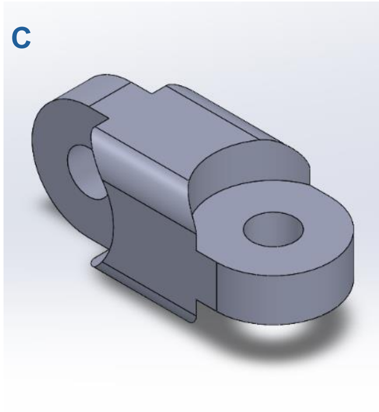

FIG 44 (A,B&C): V1 PP

V2:

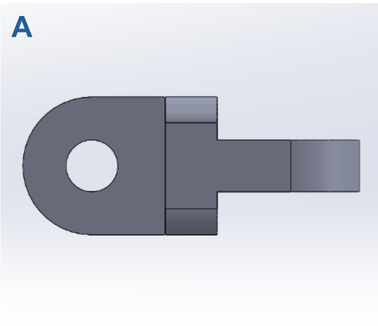

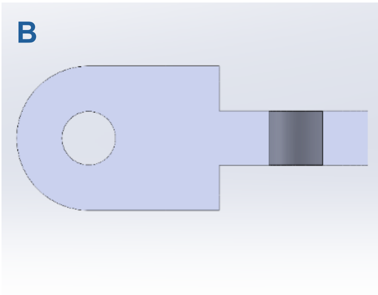

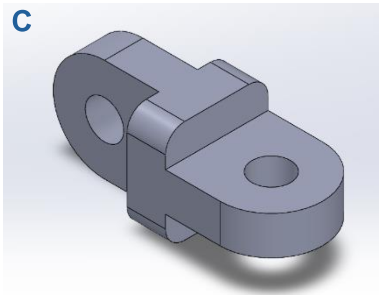

FIG 45 (A,B&C): V2 PP

V3:

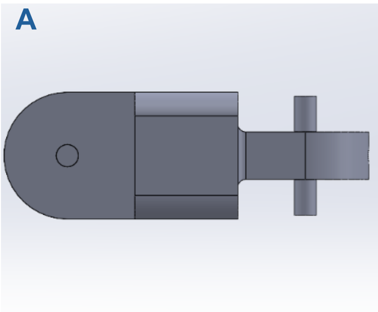

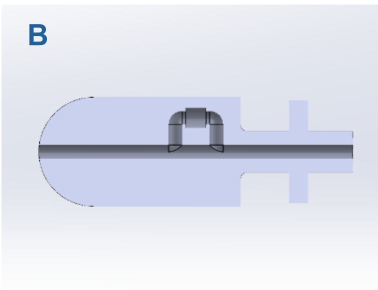

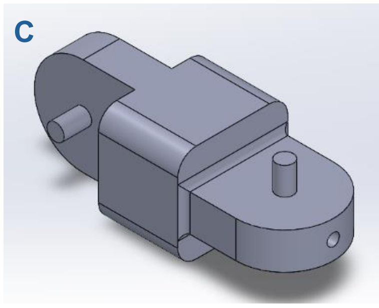

FIG 46: (A,B&C) V3 PP

V4:

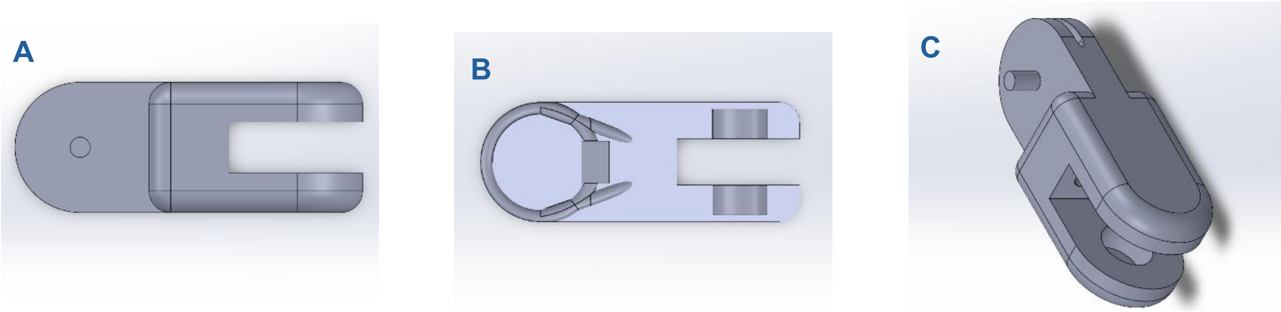

FIG 47 (A,B&C): V4 PP

V6:

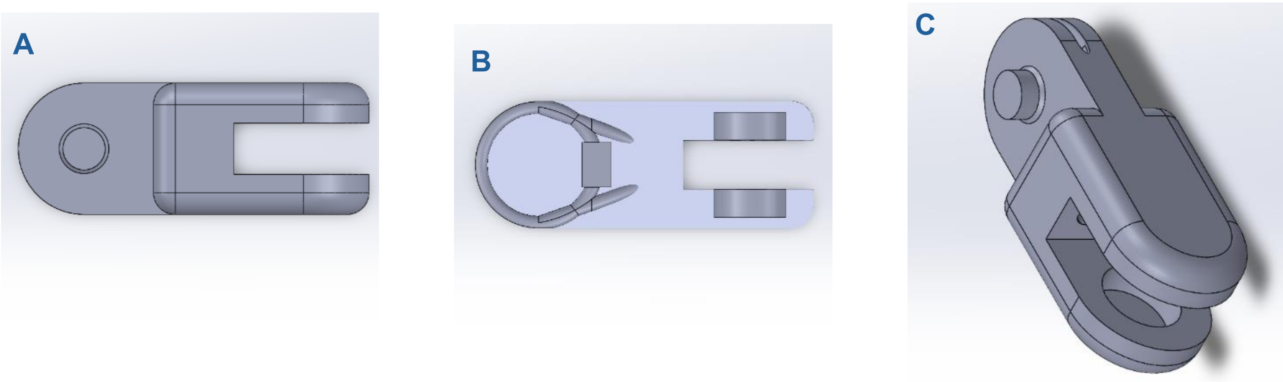

FIG 48 (A,B&C): V6 PP

11.5 Carpal architecture and tendon routing

V1:

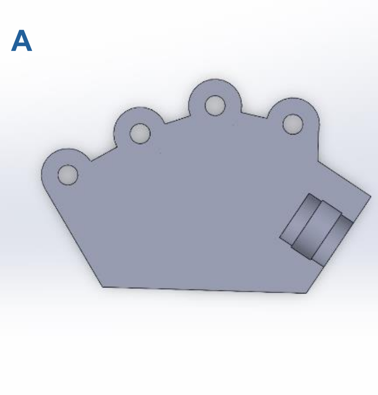

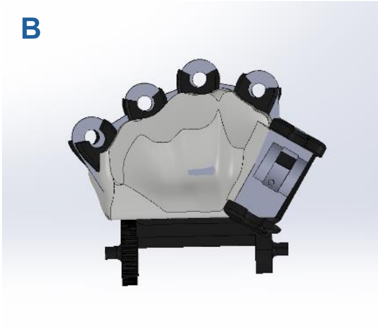

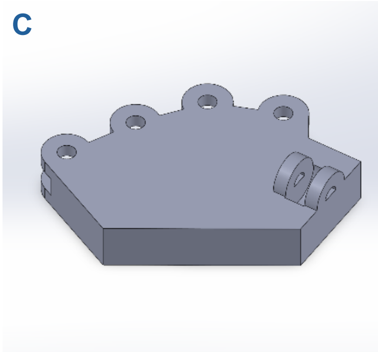

FIG 49 (A,B&C): V1 Carpal

V2:

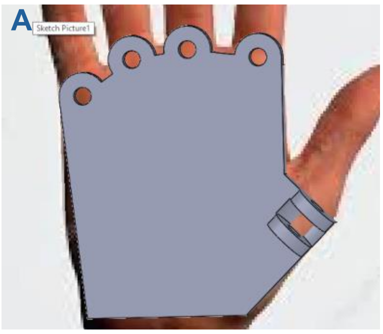

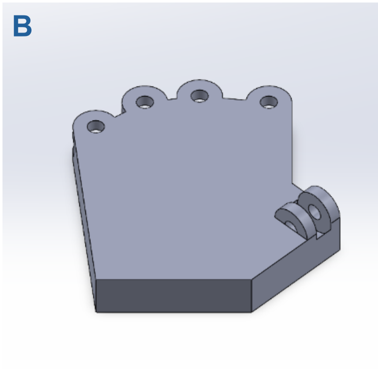

FIG 50 (A&B): V2 Carpal

V3:

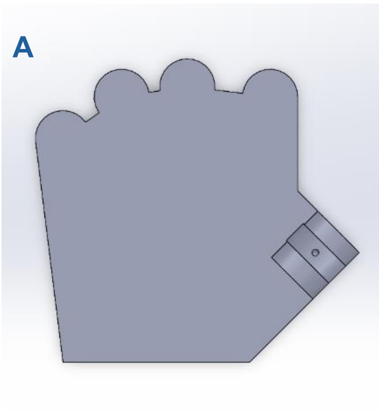

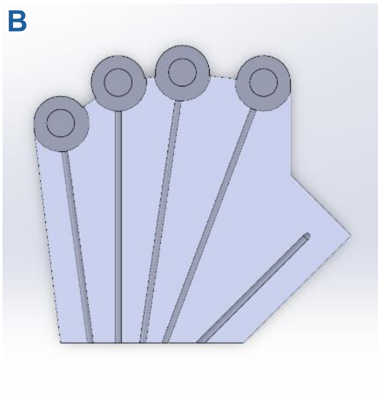

FIG 51 (A&B): V3 Carpal

V4:

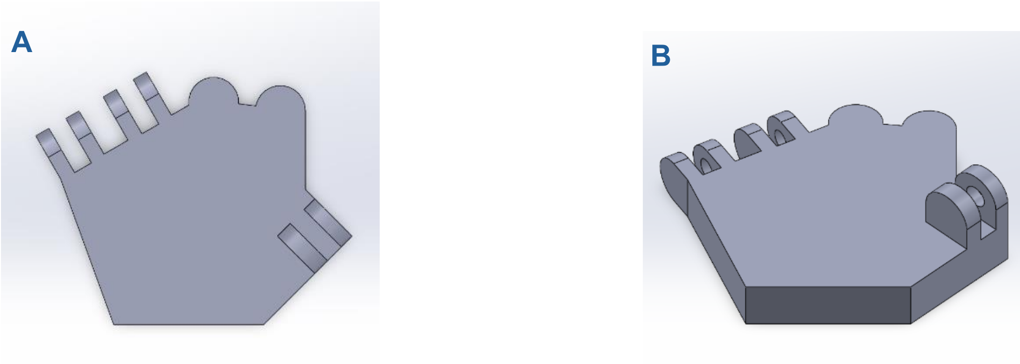

FIG 52 (A&B): V4 Carpal

V5:

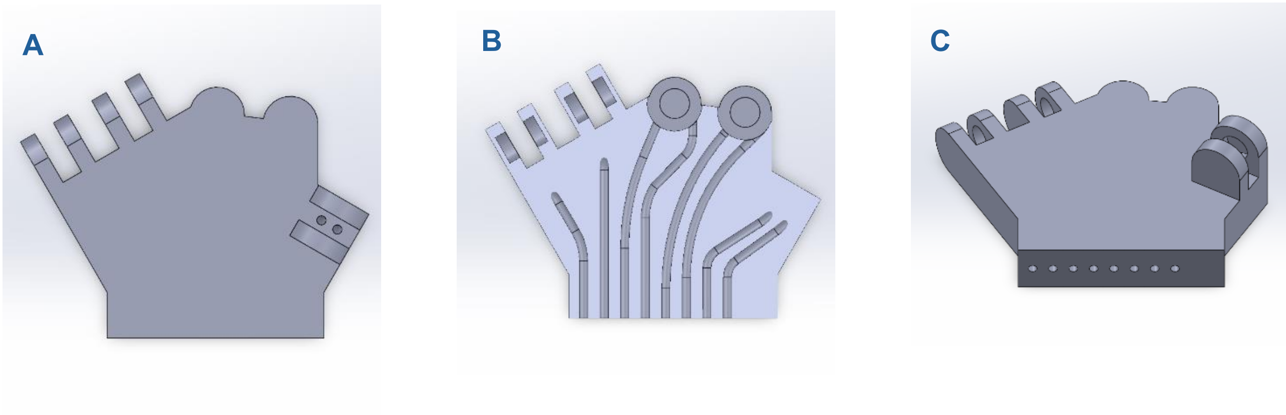

FIG 53 (A,B&C): V5 Carpal

V7:

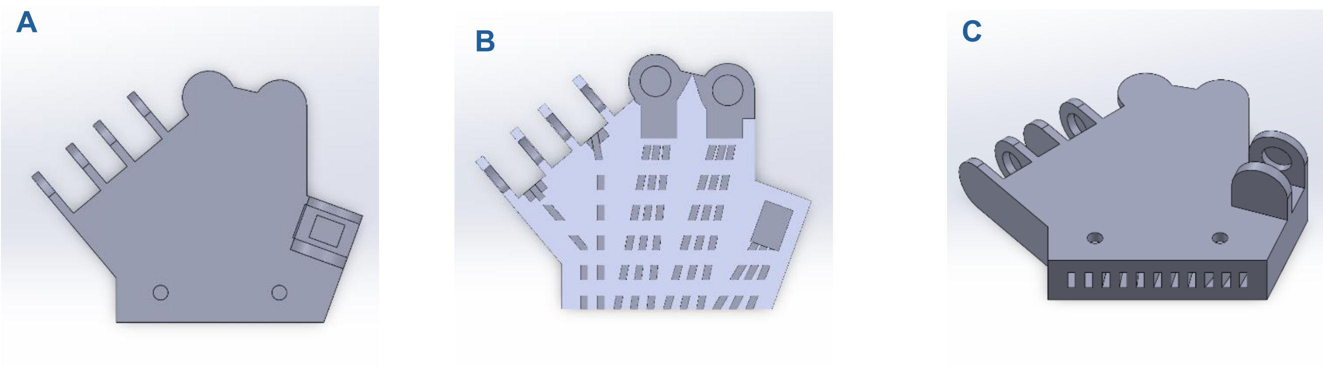

FIG 54(A,B&C): V7 Carpal